NASACR-159,306

NASA-CR-159306
19800023897

NASA Contractor Report 159306

Laser Angle Measurement System

C.R. Pond, P.D. Texeira,
R.E. Wilbert
Boeing Aerospace Company
Seattle, Washington 98124

Contract NAS1-15410
October 1980

NASA
National Aeronautics and
Space Administration
Langley Research Center
Hampton, Virginia 23665

NASA Contractor Report 159306

Laser Angle Measurement System

C.R. Pond, P.D. Texeira,
R.E. Wilbert
Boeing Aerospace Company
Seattle, Washington 98124

CONTRACT NAS1-15410
October 1980

NASA

N80-32405#

TABLE OF CONTENTS

LIST OF ILLUSTRATIONS

INTRODUCTION

This document is the final report on contract NAS1-15410. The document covers the system configuration, operation, alignment, and maintenance, together with the result of a demonstration test at the NASA-Langley 8-ft transonic wind tunnel.

The developmental breadboard Laser Angle Meter (LAM) as delivered under this contract is similar in principle to equipment now in use at the Boeing 8-ft transonic wind tunnel, but the system parameters and physical arrangement have been adjusted to suit NASA requirements.

SYSTEM DESCRIPTION

The Laser Angle of Attack Meter (LAM) is basically a fringe counting interferometer designed to measure the pitch attitude of a model in a wind tunnel. The laser source and detector circuitry are mounted above the model. Interference fringes are generated by a small passive element on the model. The fringe count is accumulated and displayed by a processor in the wind tunnel control room.

The Boeing LAM system is the first successful laser angle of attack meter for use in a large transonic wind tunnel. The LAM is the result of several years of in-house work on techniques for making high precision angle measurements through the turbulent air of a wind tunnel. The system contains several novel features that are described in this document. (An application has been filed for appropriate patent protection).

The Boeing LAM is a real-time angle measurement system, capable of measuring dynamic motion of wind tunnel models. Conventional angle measurement systems now used for wind tunnel work employ integration of about 1-second, so dynamic behavior is not observable. The fast response of the LAM also opens up possibilities for closed-loop servo techniques to set model attitude, resulting in wind tunnel cost savings through decreased run time requirements. The passive element on the model is a further advantage as there are no wires to break or short.

Specifications

The important specifications of the LAM are listed in Table I below.

Table I - Laser Angle Meter Specifications

Angle Measurement	
Fringe angle	0.24 degrees
Angular resolution	0.01 degrees
Maximum angle rate	140 degrees/sec
Angular range	±20 degrees
Physical Characteristics	
Output beam diameter	10-cm
First order offset angle	0.5 degrees

Optical Assembly

The optical assembly contains the laser beam projection optics, optical detection circuitry, and buffer amplifiers to drive the cable connecting the optics and the signal processing electronics. The optics are packaged in a heavy wall aluminum tube. All of the optics, with the exception of the large collimating lens, are mounted on a single plate. The plate can be easily removed for servicing the laser or buffer amplifiers. A port in the side of the tube provides access for checking alignment.

Figure 1 is a sketch of the optical assembly as viewed through the access port. The laser is a standard 4.44 cm diameter low power helium-neon laser. The negative lens mounted on the laser is used to control the beam divergence. The beam reflects off the pair of alignment prisms and illuminates the mask and diffuser assembly. The position of the laser spot on the mask and diffuser is critical, and must be checked when a new laser is installed. (See the section on alignment).

The radial grating is a plastic replica of a standard code disc. The grating is rotated at 3600 RPM by the motor. The moving grating next to the diffuser generates a set of moving diffuse sources at the focal point of the large collimating lens (not shown). The angular spacing of the beams from adjacent grating openings is equal to the fringe angle of the retroreflector assembly on the model.

The beam from the retroreflector assembly returns at an angle of 0.5 degrees to the outgoing beam. This offset return beam strikes a 45 degree mirror as shown. The vignetting that would occur in the signal relay optics is eliminated by use of a field lens that images the exit aperture of the optical assembly onto the entrance aperture of the signal relay optics. The signal relay optics contains a collimating lens, a 30 nm bandpass filter,

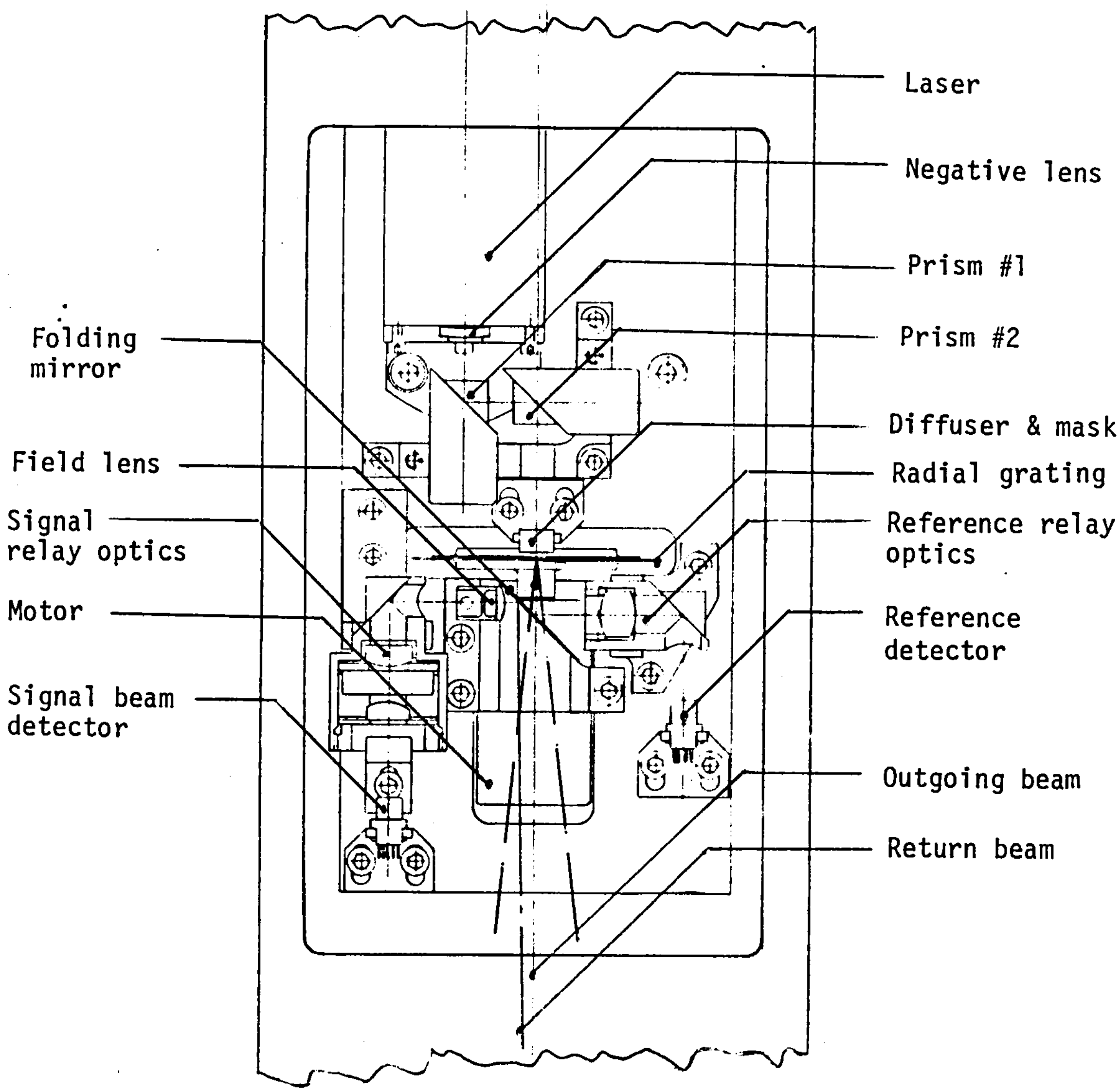

Figure 1 - View of optical assembly with side access cover removed.

and a focusing lens. The beam is finally focused onto the signal beam detector.

The output of the signal detector is a nominal 6 KHz voltage, where the phase varies with the angular position of the retroreflector assembly. A phase variation of 2π occurs for each 0.24 degrees change in the pitch attitude. This voltage is applied to one of the buffer amplifiers on the optical assembly plate.

Part of the light from the grating and diffuser is reflected off the back of the folding mirror and imaged onto the reference detector. The output of the reference detector is a fixed 6 KHz voltage. As explained later in more detail, the change in pitch attitude is determined by measuring the change in phase between the signal and reference voltages.

Retroflector Assembly

Figure 2 shows the components of the reflector assembly. The basic elements are a retroreflector and a linear grating positioned behind a window. The window is hot formed to match the external contour of the model.

The retroreflector shown in the figure is a cube corner retroreflector. The essential property of the retroreflector is that the incident and exit beams are parallel. Just as a ball thrown near a corner will bounce off two walls and the floor then return, the light reflects off the three facets of the cube corner and exits in the direction of the source.

The hologram is a linear grating manufactured by a holographic process. The hologram is bleached to increase the diffraction efficiency. An index matching fluid (canada balsam) is used between the hologram and the retroreflector to reduce Fresnel reflection losses.

The input beam is diffracted into two first order beams by the hologram as shown in Figure 2-a. For this discussion, consider only the +1 order beam. When the zero order beam passes back through the hologram, another +1 order beam is produced. This pair of beams is parallel. Optical interference occurs over the superimposed beams, where the intensity is maximum when they are in phase and minimum when they are out of phase.

The phase difference between the +1 order beams depends on the input beam angle. Figure 2-b illustrates the angular dependence of the first order results from optical interference of the beams. The sinusoidal pattern repeats every 0.24 degrees. The phase of the 6 KHz signal varies with pitch attitude. The change in phase is measured and displayed by the electronic processor.

Electronics

Figure 3 is a block diagram of the electronics for the angle measurement system. The electronics is housed in two separate assemblies, the optical

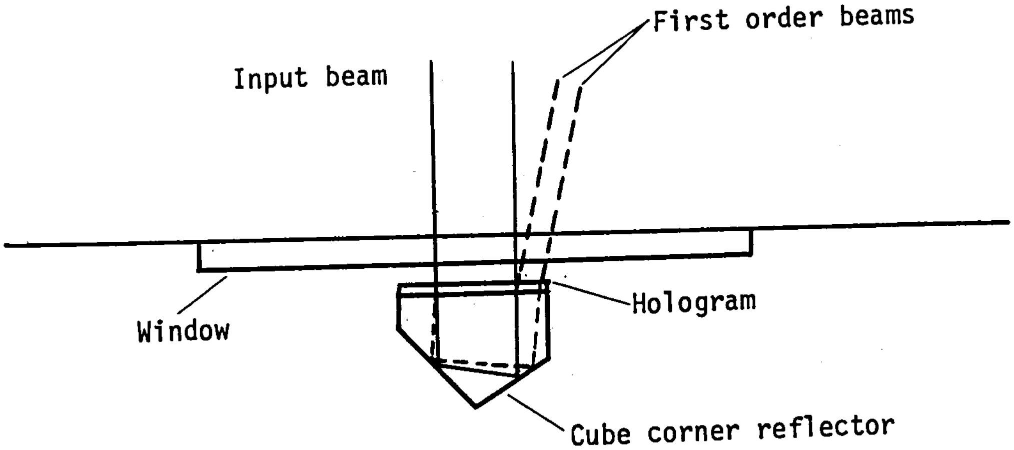

(a) Schematic showing geometry of interfering beams

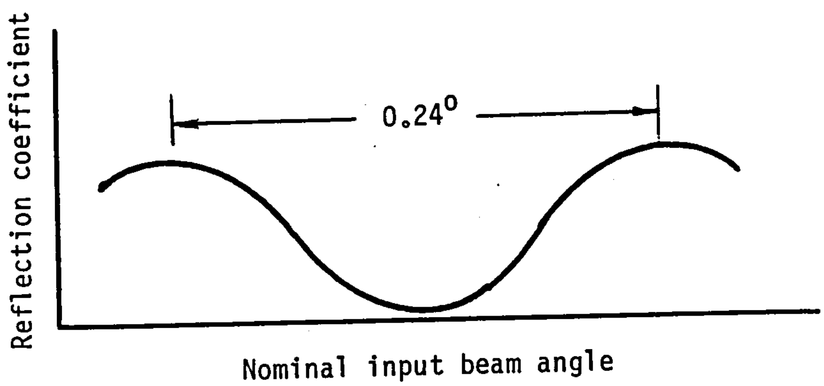

(b) Reflection at reflector assembly versus input beam angle

Figure 2 - Retroreflector assembly

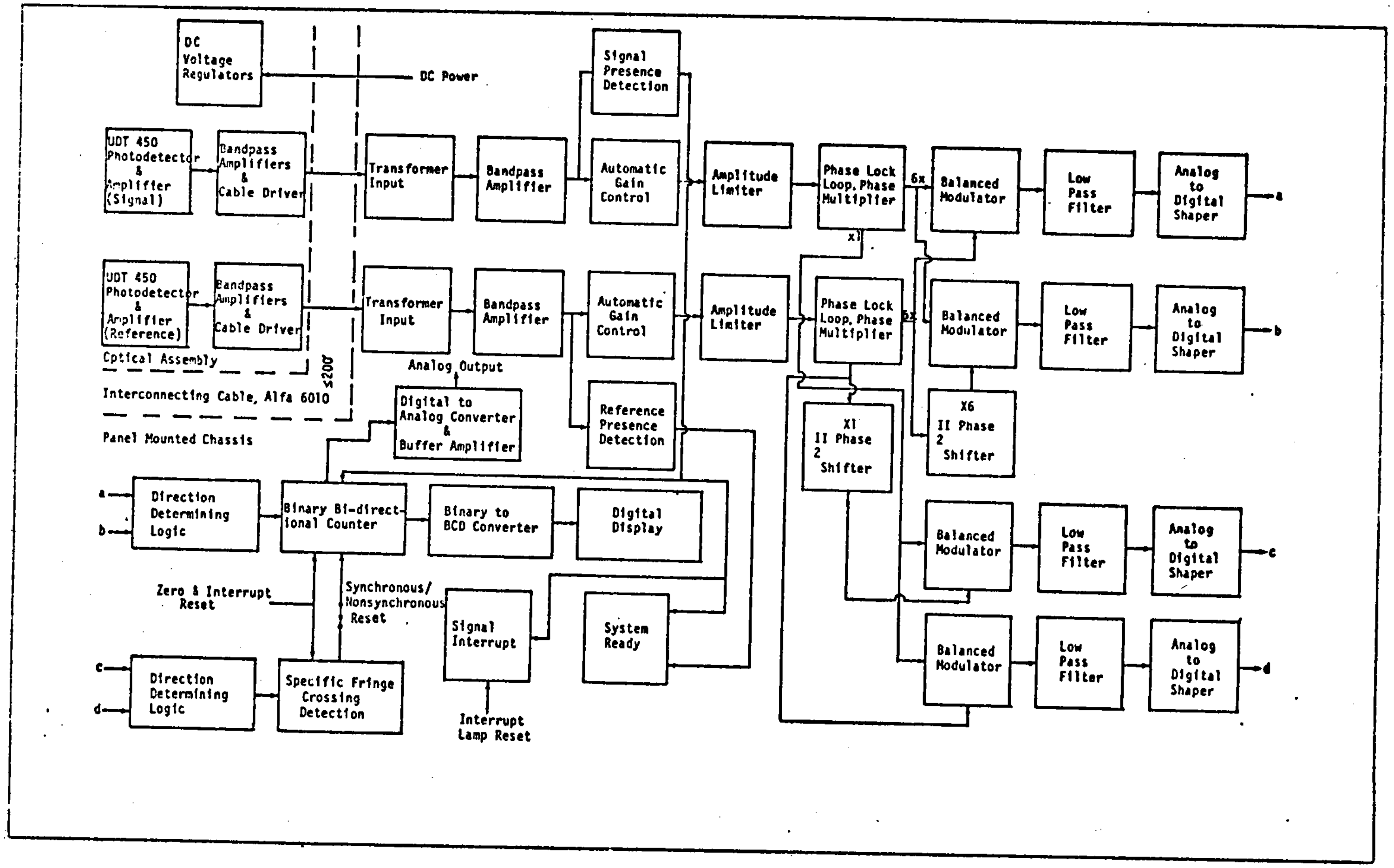

Figure 3. Electonics block diagram.

assembly and the panel mounted chassis assembly (signal processor). The two units are connected together by a cable.

Two alternating electrical voltages are generated by photodetectors in the optical assembly. The generation and significance of these two voltages have been described in the optical section. To obtain relative angular measurement, phase measurement must be continuously made between the 6 KHz reference voltage at the reference detector and the 6 KHz phase varying signal at the signal detector.

The electronics in the optical assembly consists of the signal channel and the reference channel. Each channel has a United Detector Technology, Inc. UDT-450 light to voltage converter which consists of a silicon photo-diode and a low noise current mode operational amplifier in the same package. Since the reference is generated within the optical assembly it does not require as much amplification as the signal channel. The signal channel UDT-450 is followed by a low noise amplifier resulting in a noise figure determined by the UDT-450. The bandpass filters in the optical assembly are second-order-multiple-feedback operational amplifier band-pass filters with a bandpass of 2.4 KHz at the 3db points. These operational amplifiers are also the cable drivers.

The cable, Alfa 6010, has three shielded twisted pairs and a ground. Low voltage d.c. power for the electronics in the optical assembly is provide from the panel mounted chassis assembly through this cable. Voltage regulators are used at the optical assembly for decoupling. The other two twisted pairs are used to transmit the reference phase and received signal from the optical assembly to the processing electronics in the panel mounted chassis.

At the signal processor the reference and signal twisted pairs terminate at transformers minimizing ground loops and pickup in transmission of these signals for distances up to 200 feet. The bandpass amplifiers following the transformers are also second-order multiple-feedback operational amplifier bandpass filters with a bandwidth of 3 KHz at the 3db points.

The signal and reference presence detectors consist of a full wave envelope detector and Schmitt trigger with adjustable thresholds. The attack time is limited by the bandwidth of the signal and reference channel respectively, as seen at the output of the bandpass amplifier, and the decay time is determined by the time constant of the envelope detector. Signal presence is indicated on the front panel by a lamp. The signal presence detector also keeps the counter from counting when signal is not present and the signal presence also activates the system ready lamp when both signal and reference are present. After the processor is reset, an interruption of the signal activates a lamp on the front panel. The interrupt lamp can be reset by the lamp interrupt reset switch on the front panel. This switch resets only the interrupt lamp. The zero reset switch resets the counter to zero and also resets the interrupt lamp.

The automatic gain control circuits have a useable dynamic range of 50db. AGC starts for an input of 25 millivolts peak-to-peak maintaining the output at 1.4 volts peak-to-peak. The circuit has an attack time of 1 to 2 milliseconds and a decay time of 0.4 sec. AGC is necessary in the signal channel to maintain a relatively constant input to the multiplier circuits for the large dynamic range of the input to the processor due to different retroreflectors, fog, and reduced laser output because of laser aging. AGC is used in the reference channel primarily because of laser aging. Operational amplifier diode limiters follow the AGC circuits to limit the instantaneous amplitudes of the signal and reference signals before application to the phase multiplication circuitry.

The retroreflector assembly fringe angle is 0.24°. Electronic phase resolution of 1/24 cycle is required for an optical resolution of 0.01°. A factor of four results from standard quadrature phase detection and a factor of six results from frequency multiplication before phase detection. Multiplication is accomplished by insertion of a divide down counter in a Phase Lock Loop, PLL. Multiplication of twelve is used within the loop but six times the input phase is used as the output of the PLL. It was necessary to divide the multiplied output of the voltage controlled oscillator by two to obtain a symetrical wave shape at six times the input phase before phase comparison by the balanced modulators.

Since the phase change of the signal is bidirectional, relative to the reference signal, quadrature signals are generated using two balanced modulators to enable determination of the direction of phase change and the instantaneous total phase. This is done for the mulitiplied and unmultiplied signals and references. The unmultiplied signal is the PLL divided signal, phase locked to the input of the PLL. Note that the signal is applied to both balanced modulators but the reference is shifted in phase by $\frac{\pi}{2}$ radians to one of the balanced modulators. Each balanced modulator multiplies the inputs applied to it. The output of the balanced modulators after filtering by the low pass filters represent phase of the signal relative to the reference as a function of time. Since phase information is preserved in multiplication by the balanced modulators the output of the balanced modulator pairs is quadrature.

Sixth order Butterworth active filters are used for the low-pass filters. The analog-to-digital shapers change the analog output of the active filter to digital levels. The shaper consists of a Schmitt trigger with adjustable hysteresis.

Waveshapes for a constant rate of change of phase for the signal relative to the reference (constant angular rate of change of the retroreflector) are shown in Figure 4a. Note that the square waves at a and b are in quadrature and have six cycles for each cycle at c and d, which are also in quadrature. Figure 4b is a representation of the possible states (logic levels) for a pair of quadrature signals. Notice a repetitive sequence exists. Assume at some instant in time a is zero and b is zero. If the phase difference is increasing the next state for a is one and b would be zero. If the phase difference is decreasing the next state for a is zero and b would be one. Examination of the sequence reveals that by knowing the previous level determination of an increase or decrease of phase can be made. It is important to note that each 1/4 cycle of the quadrature signals are now identifiable. Thus it can be seen that by phase multiplication of six and processing of the quadrature signal by the direction determining logic, phase changes of $\frac{\pi}{12}$ radian are resolved. Without the phase multiplication, phase changes of $\frac{\pi}{2}$ are resolved. The direction determining logic for the unmultiplied signal is used with other circuitry to identify a specific zero

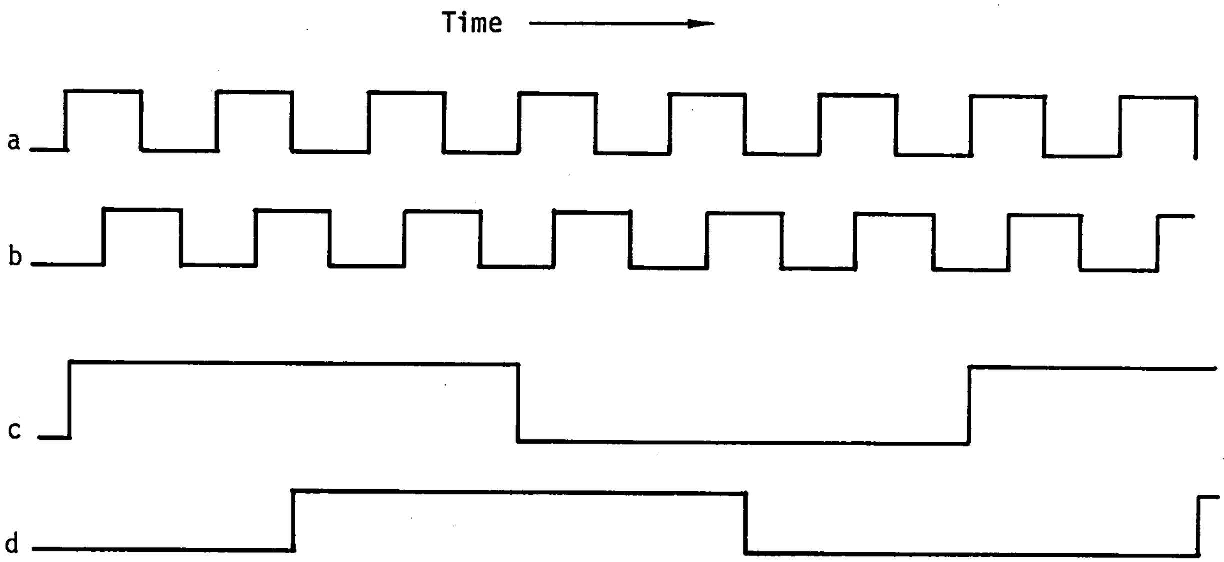

(a) Quadrature waveforms for a constant rate of phase change between the signal & reference.

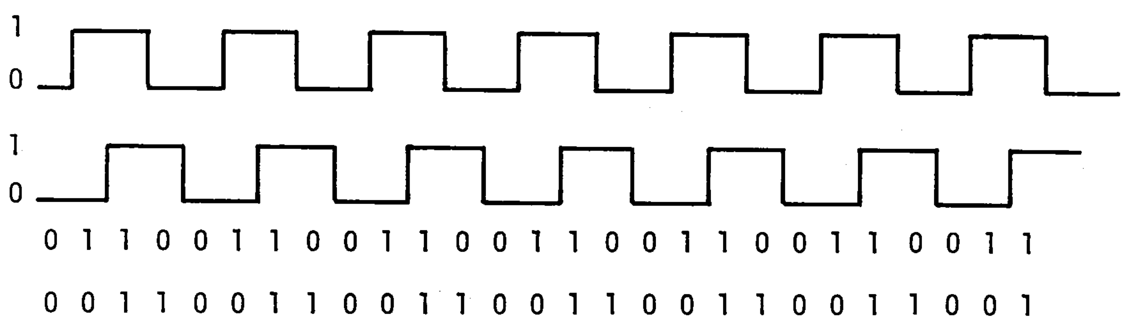

(b) Representation of logic levels for quadrature waveforms.

Figure 4. Quadrature waveforms.

crossing and to start the counter at this crossing. A switch is located on card #4 to switch from this mode (called synchronous reset) to non synchronous reset mode where reset occurs instantly without regard to a specific zero crossing. The direction determining logic for the multiplied signal has two outputs that go to the bidirectional binary counter. A pulse appears for each $\frac{\pi}{12}$ radian change in phase of the signal relative to the reference, one output for increasing and the other for decreasing phase changes.

The counter is a twelve bit binary bidirectional counter driving a Datel DAC HR 13B digital to analog converter, DAC, and a binary to BCD converter. The 12 most significant bits of the DAC are used. The analog output range is $\pm$10 volts with each quantized step equal to 4.88 millivolts. The binary to BCD converter drives the digital display on the front panel which represents counts divided by 100. Each count on the digital display and each quantizing step of the DAC represents approximately an angle of .01 degrees.

MAINTENANCE

This section lists the components that will require periodic maintenance and outlines replacement and alignment procedures. Before replacing any component, read the section "SYSTEM DESCRIPTION" and study the appropriate schematics and drawings so that you understand the function of the component.

Optics

Caution - Do not disturb any optical elements except those noted below. Complete alignment is a time consuming process that requires several pieces of special equipment available only in a well-equipped laser laboratory. The only elements that may have to be replaced are the laser, the synchronous motor, the code disc, and possibly the optical detectors.

Laser Replacement

1. Remove the optical assembly as outlined under "Optical Assembly Removal".

2. Remove the two laser hold-down clamps.
3. Remove the negative lens attached with four 4-40 screws on the output end of the laser.
4. Mount negative lens on new laser. (The concave side of the lens is toward the laser).
5. Install new laser, tighten hold-down clamps. The rotation of the laser is not important. The laser output end should be in the approximate position shown in Figure 1.
6. Install optical assembly in optical tube.
7. Align new laser with optics as described below.

<u>Optical Alignment of Prisms #1 and #2</u>

Prisms #1 and #2 are used to position the laser spot on the diffuser. Proper alignment is very important, as both signal and reference channels are affected.

1. Place the optical assembly so that the internal mounting plate is horizontal, with the access port on the upper side of the tube.
2. Turn the motor on. (The switch is at the end of the optical plate).
3. Turn the laser on.
4. Adjust prism #1 to align the laser beam with the rotation axis of prism #2.
5. Center the laser spot on the diffuser aperture by rotating and translating prism #2. Avoid contact with the plastic code disc and prism surfaces.
6. Set up a retroreflector assembly on a mount that allows horizontal translation across the center of the 10-cm output beam and rotation about a vertical axis. The reflector should be within 10-cm of the output lens.
7. Attach the cable from the optical assembly to the processor. Turn the processor on.
8. Connect an oscilloscope to the BNC outputs (signal and reference) at the end of the optical assembly.
9. Adjust the spot position at the diffuser by rotating and translating prism #2 to produce maximum signal output. This is a broad

maximum. Then adjust prism #2 to bring up the reference level, keeping the signal level near the maximum value. Translate the reflector over the beam to make sure that the signal level is approximately uniform and the envelope (resulting from reflector rotation) is less than 30% over the output beam. Envelope modulation causes small scale angle nonlinearity. If the envelope modulation is excessive, readjust the prism to decrease the reference level.

Optical Assembly Removal

The optical assembly is removed in the following steps:

1. Disconnect electrical connectors at back plate.
2. Remove cover plate from side of housing tube.
3. Remove 2 cap screws located opposite cover plate.
4. Remove 4 cap screws holding back plate to housing.
5. Loosen 2 cap screws holding optical plate to back plate.
6. Remove optical assembly by lifting front end of optical plate and forcing to the rear. Careful use of a wooden pry bar on the end of the optical plate will assist in its removal.

Synchronous Motor Removal

The motor mounting bracket is attached to the bottom of the optical plate with 3 cap screws. Loosen the 2 set screws in the hub to remove the code disc holder from the motor shaft. This will expose the 2 flush screws which attach the motor to its mounting bracket.

Electronics

The electrical schematics and alignment procedures are described below.

Electrical Schematics

Figures 5 through 14 are the electrical schematics for the LAM. The schematics are arranged in the order of signal and reference flow from the optical assembly through the signal processor. A description of the 200-ft connecting cable is included.

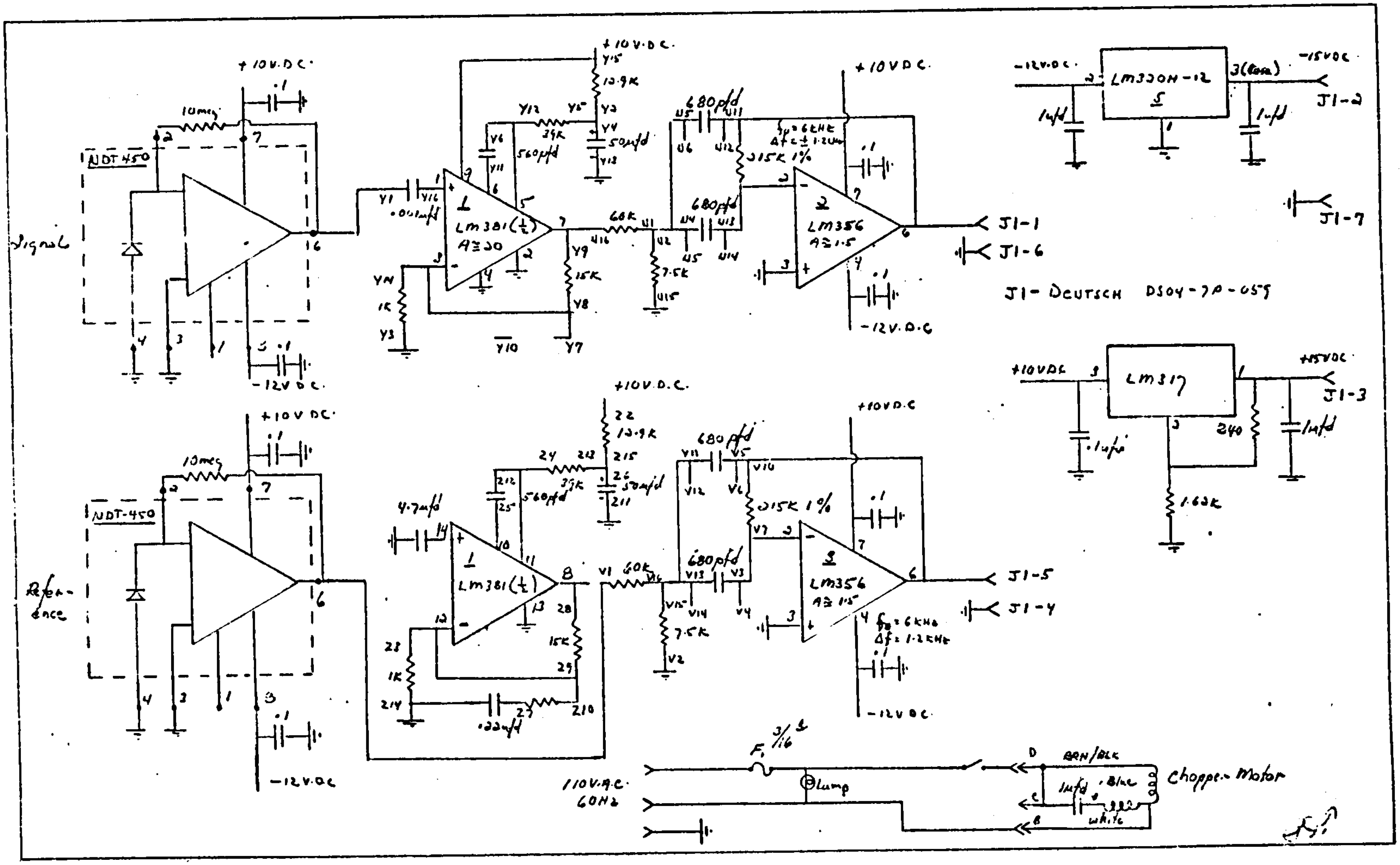

Figure 5. Optical assembly circuitry.

Cable Alfa 6010 #22 Stranded 3 pairs

Connectors - Deutsch DS07-73-059/MDR07-75-090

Connector Pin No.		Color of Wire
Pair	2	Black
	3	Red
Pair	4	Black
	5	White
Pair	6	Black
	1	Green

Shields 7

Figure 6 - Cable Between Optical Assembly and Drawer

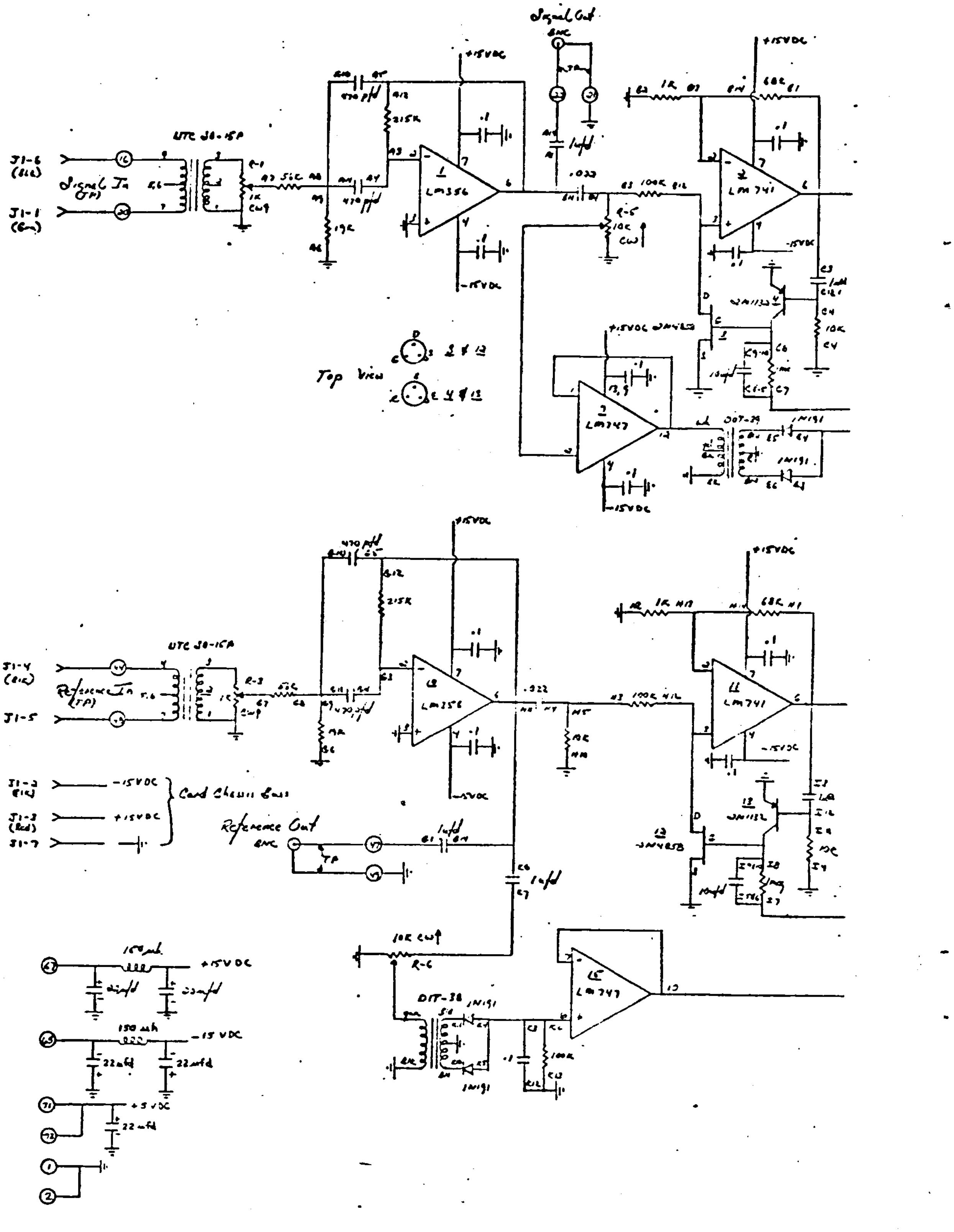
Signal Out
+15VDC
-15VDC
LM356
LM741
LM747
Top View
Reference Out
Card Chassis Bus
+5VDC
J1-6
J1-1
J1-4
J1-5
J1-2
J1-3
J1-7

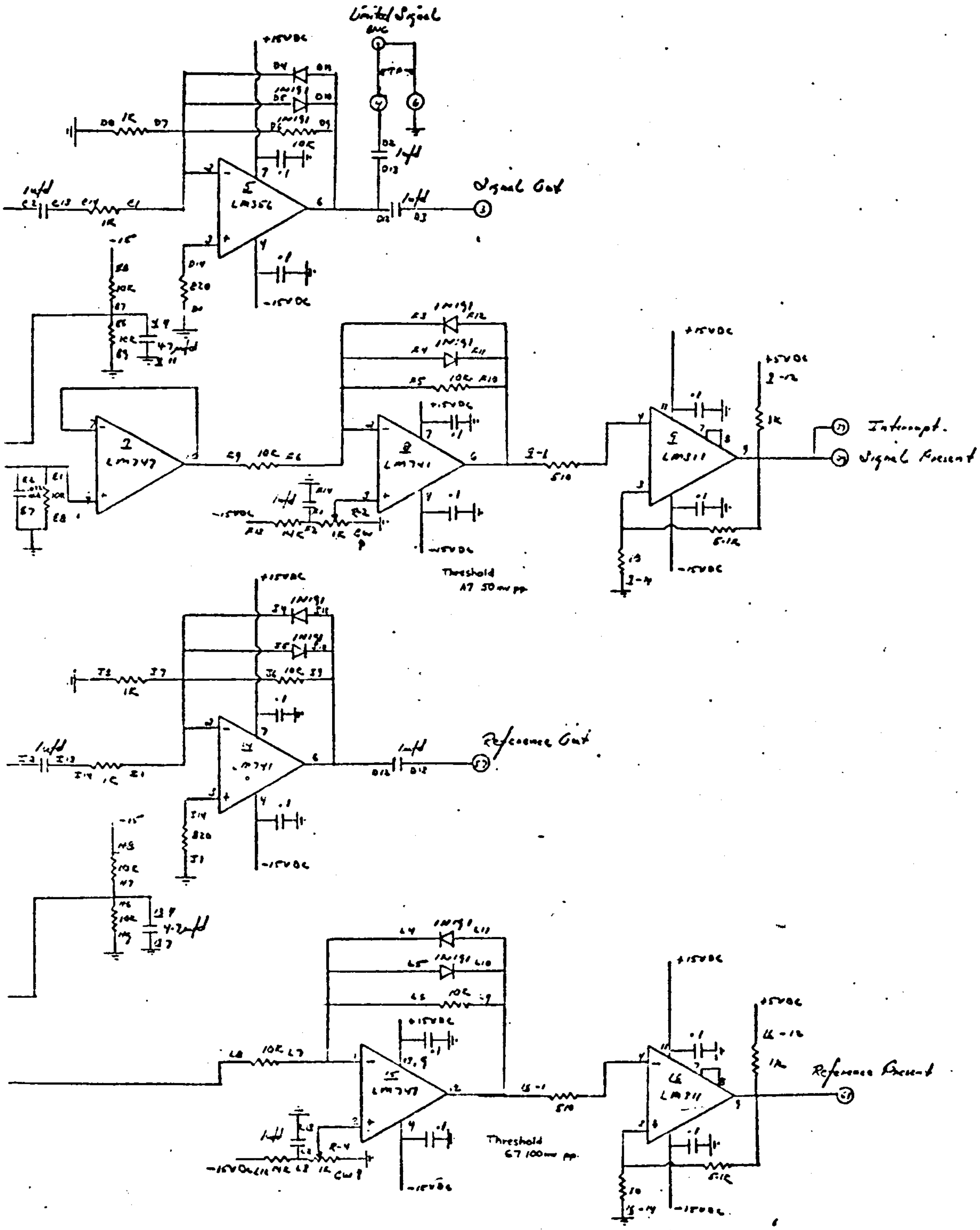

Figure 7. Card No. 1, AGC, limiting, signal and reference presence detection.

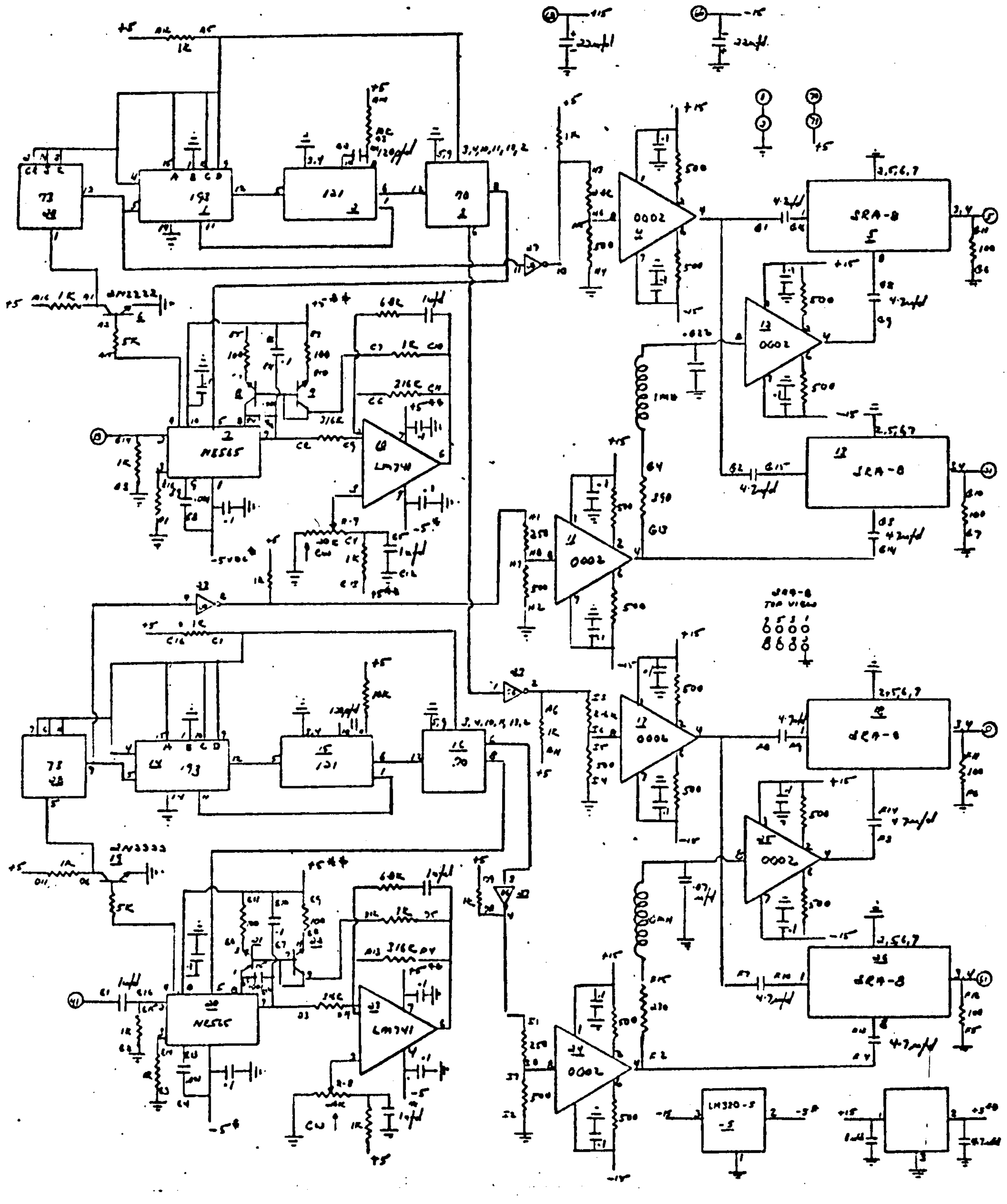

Figure 8. Card No. 2, multipliers.

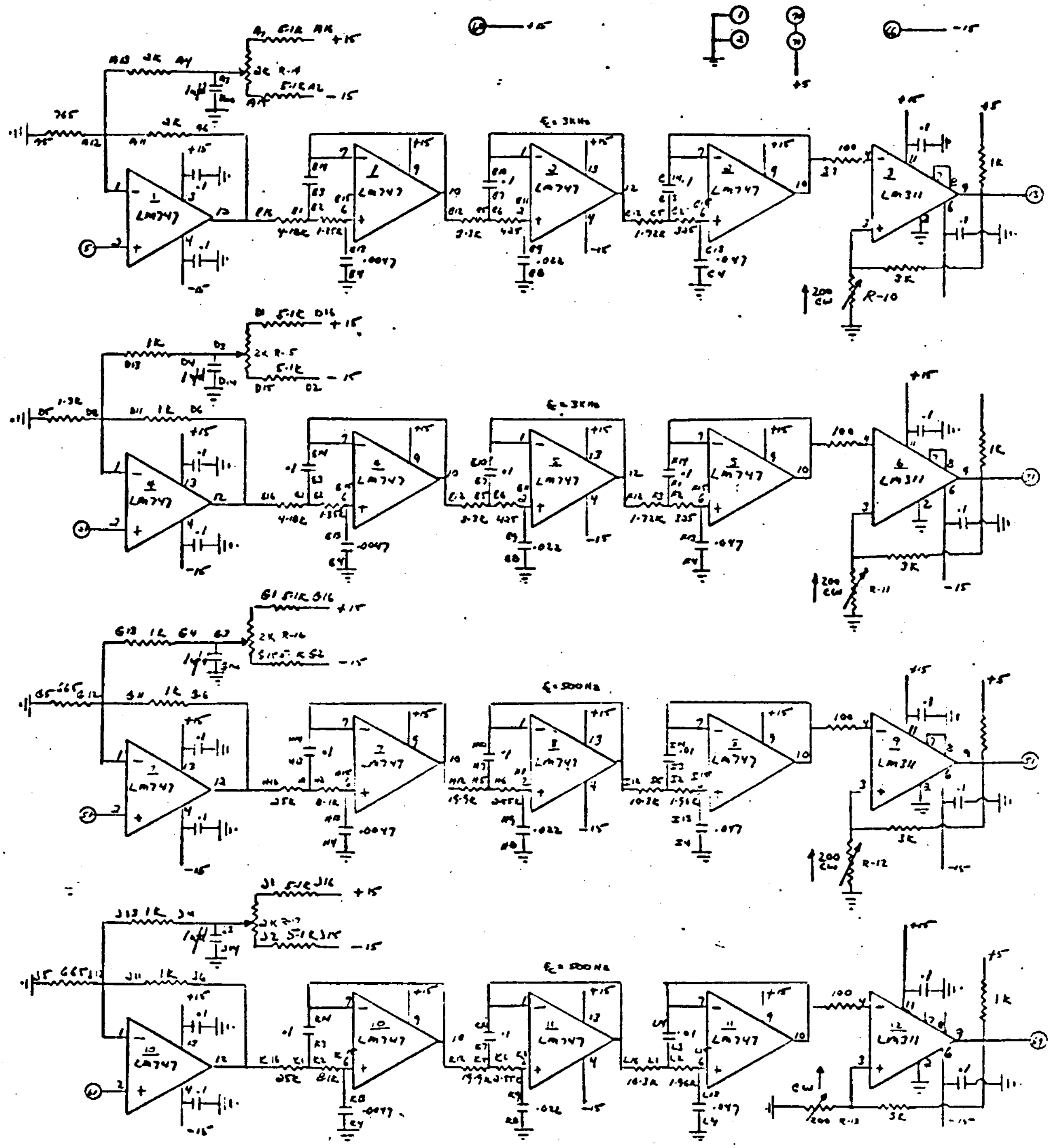

Figure 9. Card No. 3, low pass filters.

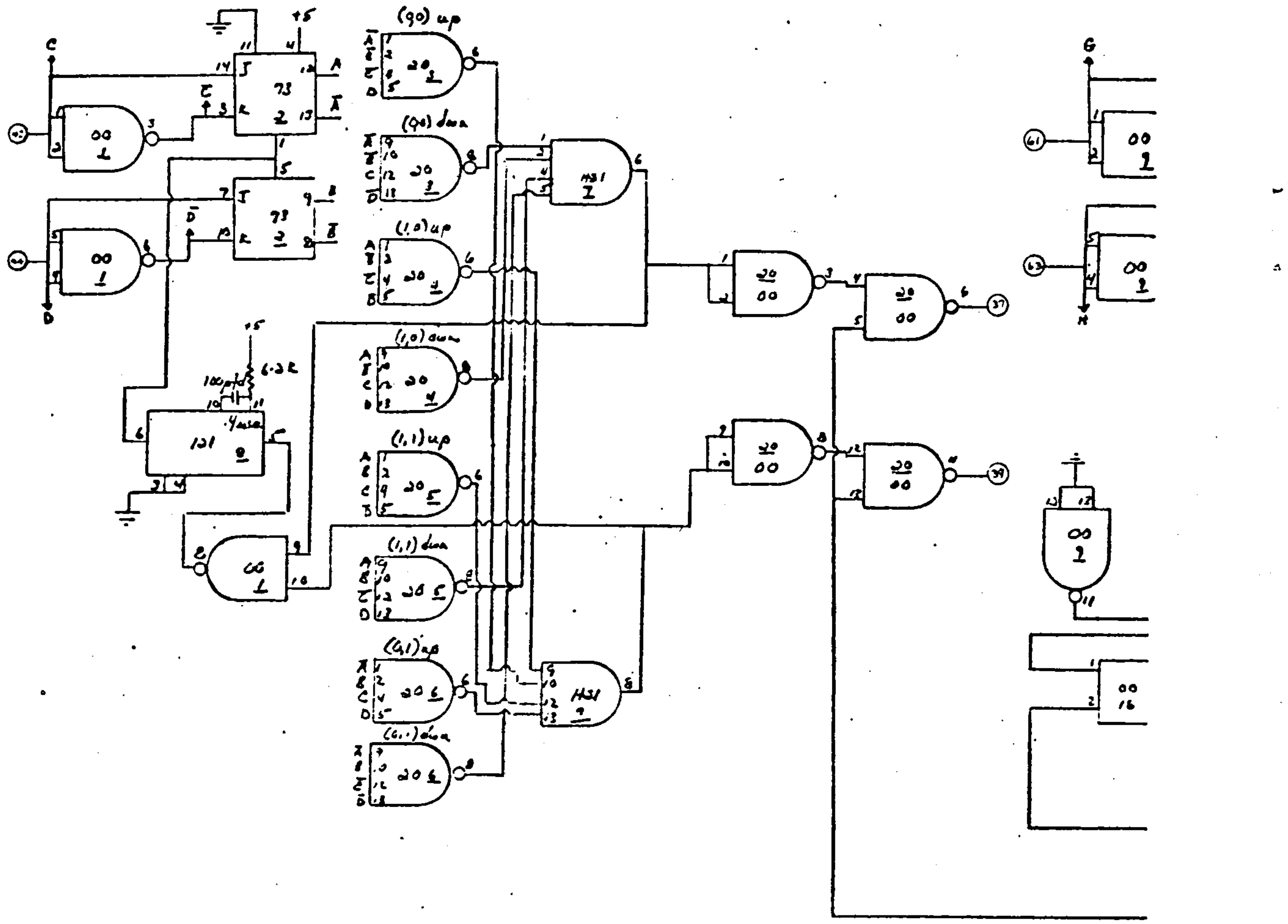
+5
73
121
(1,0) up
(1,1) up

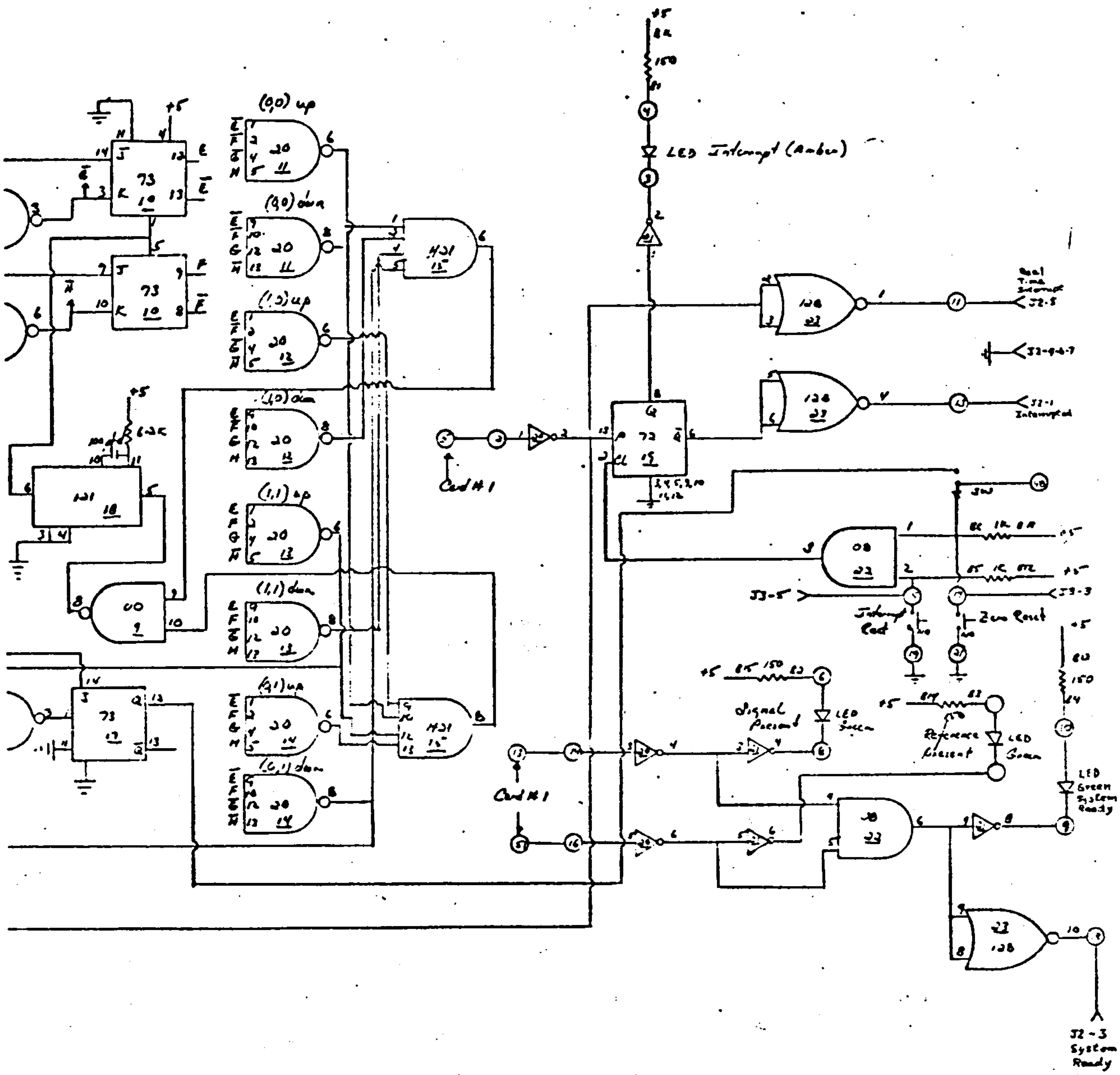

Figure 10. Card No. 4, direction determining and control logic.

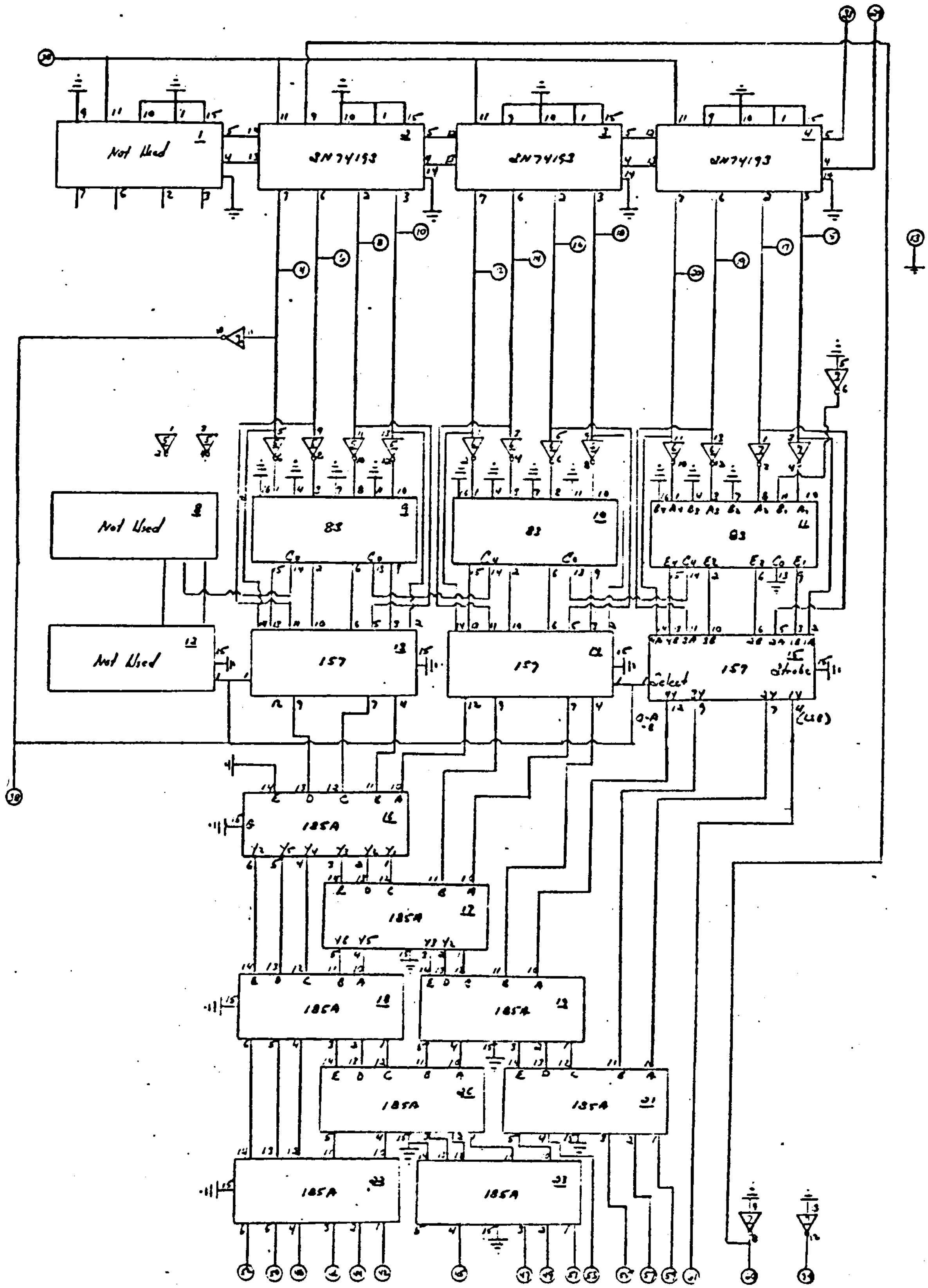

Figure 11. Card No. 5, counter and binary to BCD converter.

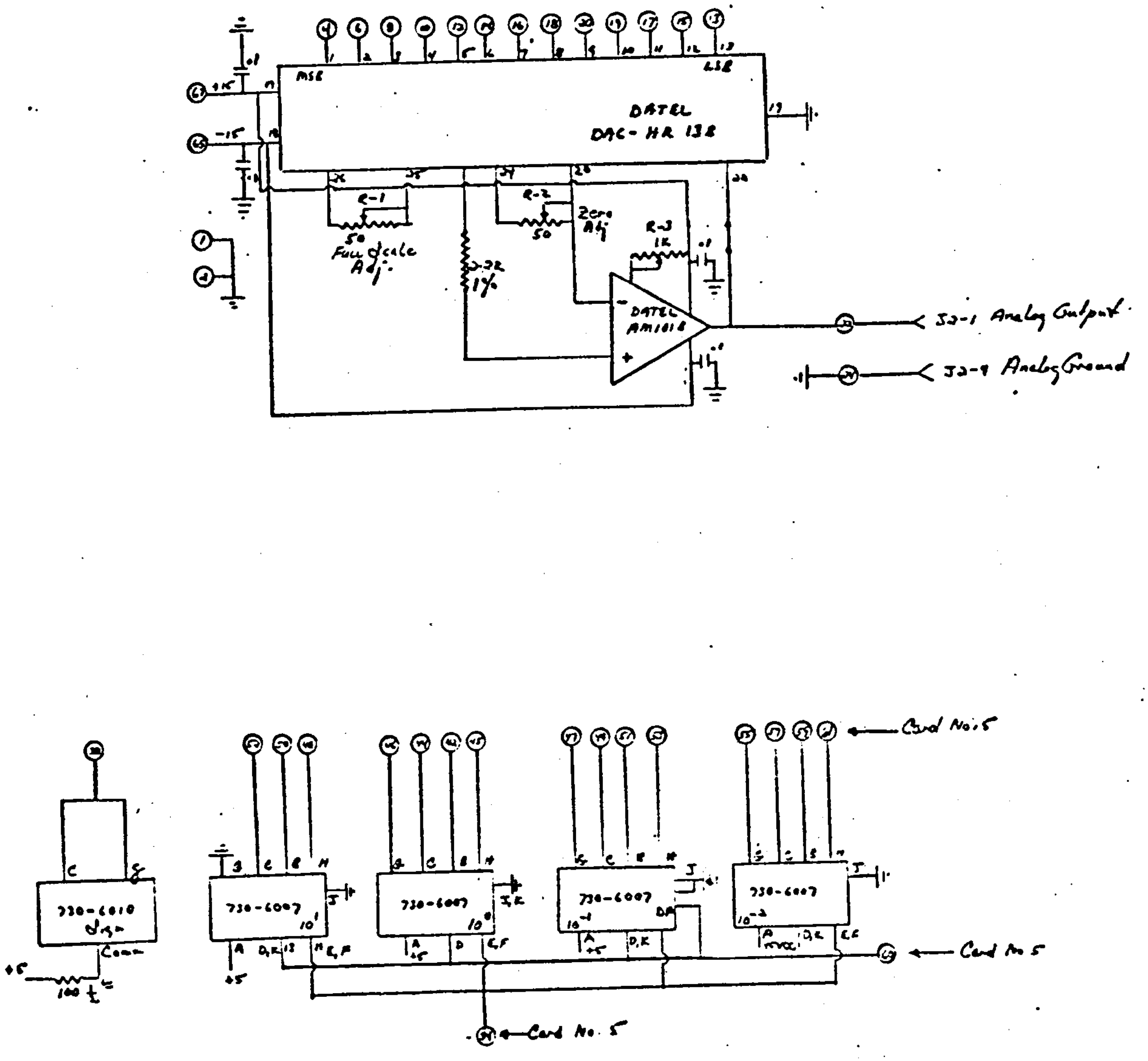

Figure 12. Digital display circuit and Card No. 6, DAC.

Card #1 conn.	Card #1 pin	Card #1	Card #2 conn.	Card #2 pin	Card #2 (Multiplier & S/H)	Card #3 conn.	Card #3 pin	Card #3 (Low Pass Filters)
	1	⏚		1	⏚		1	⏚
	2			2			2	
2-13	3	Signal Output		3			3	
BNC	4	Signal Limited		4			4	
	5		3-5	5	Fine Guard Out	2-5	5	Fine Guard In
	6	Ground		6			6	
	7			7			7	
	8			8			8	
	9			9			9	
	10			10			10	
	11			11			11	
	12			12			12	
	13		1-3	13	Signal Input	4-42	13	Fine Guard Out
	14			14			14	
	15			15			15	
(Blk) J1-6	16	Signal Input (Blk)		16			16	
	17			17			17	
	18	Shield J1-6&1		18			18	
	19			19			19	
(Grn) J1-1	20	Signal Input (Wh)		20			20	
	21	Signal BNC Ground	3-21	21	Fine Guard Out	2-21	21	Fine Guard In
BNC	22	Signal Output (BNC)		22			22	
	23			23			23	
	24			24			24	
	25			25			25	
	26			26			26	
	27			27			27	
	28			28			28	
4-12	29	Signal Intercept		29			29	
	30			30			30	
	31			31		4-44	31	Fine Guard Out
	32			32			32	
	33			33			33	
	34			34			34	
	35			35			35	
	36			36			36	
4-14	37	Signal Present		37			37	
	38			38			38	
	39			39			39	
	40			40			40	
	41		1-57	41	Reference Input	2-51	41	Coarse Guard In
	42			42			42	
	43			43			43	
(Blk) J1-4	44	Reference Input		44			44	
	45			45			45	
	46	Shield J1-4&5		46			46	
	47	Reference Output (BNC)		47			47	
(Wh) J1-5	48	Reference Input		48			48	
	49	Reference Output BNC Gnd		49			49	
	50			50			50	
	51		3-41	51	Coarse Guard Out	4-61	51	Coarse Guard Out
	52			52			52	
	53			53			53	
	54			54			54	
	55			55			55	
	56			56			56	
2-41	57	Reference Out		57			57	
	58			58			58	
	59			59			59	
	60			60			60	
4-16	61	Reference Presence	3-61	61	Coarse Guard Out	2-61	61	Coarse Guard In
	62			62			62	
	63			63			63	
	64			64			64	
	65	-15VDC		65	-15VDC		65	-15VDC (blue)
	66			66			66	
	67	+15VDC		67	+15VDC		67	+15VDC (yellow)
	68			68			68	
	69			69		4-63	69	
	70			70			70	
	71	+5VDC		71	+5VDC		71	+5VDC
	72			72			72	

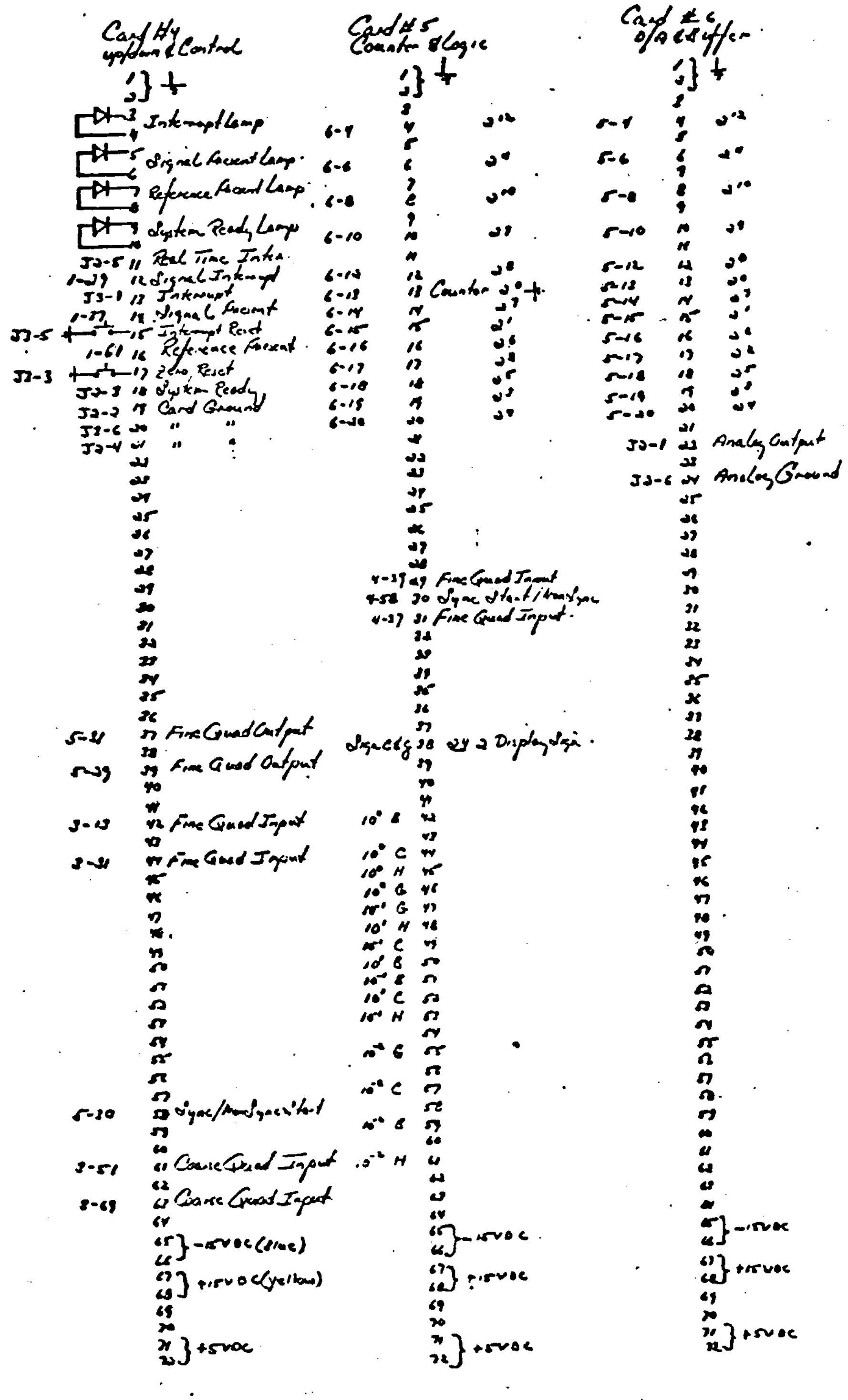

Figure 13. Card chassis wiring diagram.

Connectors

	Wire Color	Function
J1-6	Blk	Signal Input
J1-1	Grn	Signal Input
J1-4	Blk	Reference Input
J1-5	Wh	Reference Input
J1-2	Blk	-15V.D.C
J1-3	Red	+15V.D.C
J1-7	Drain	Ground
J2-3	Red	System Ready (T²L Logic 1)
J2-5	White	Real Time Interrupt (T²L Logic 1)
J2-1	Grn	Analog Output ± 10V 4.88mv/resolvable element
J2-6	Blk	Analog Ground
J2-2-4-7		Ground
J3-1	Grn	Interrupt (T²L Logic 1)
J3-3	Red	Zero Reset (1K pull up to ground)
J3-5	Wh	Interrupt Reset (1K pull up to ground)
J3-2-4-6-7		Ground
J5	BNC	Signal
J6	BNC	Limited Signal
J7	BNC	Reference

Chassis Wiring

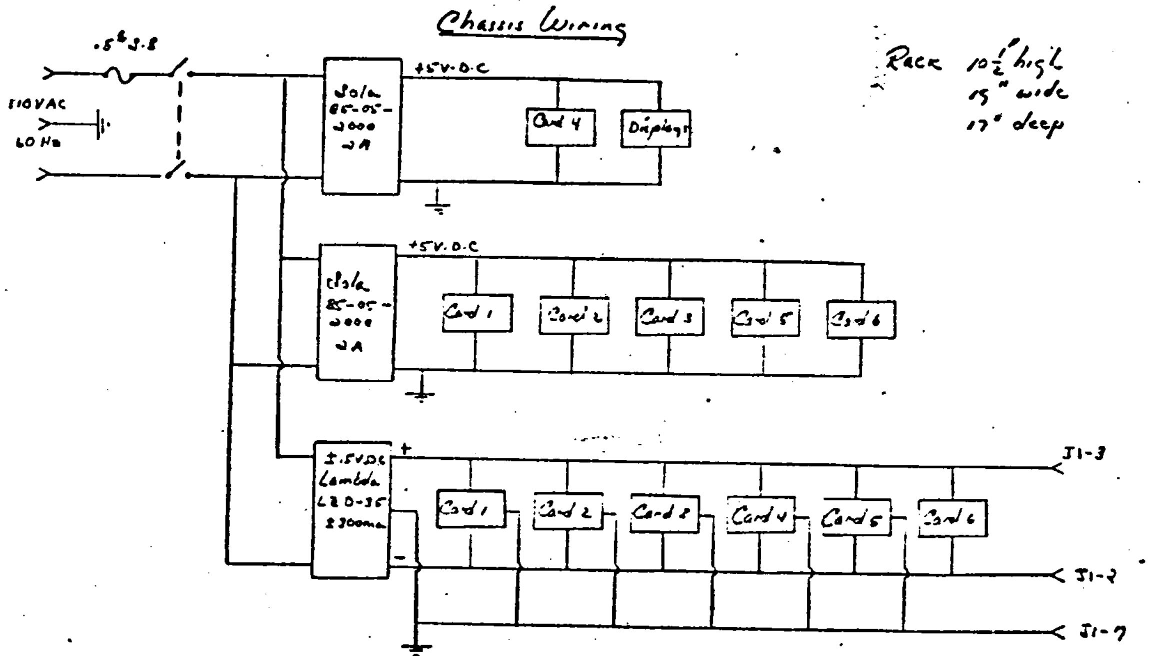

Rack 10½" high
15" wide
17" deep

Figure 14. Chassis power supplies and connectors wiring diagram.

Electronic Adjustments

Most adjustments can be made using sine wave generators for signal and reference inputs. The reference is set at 6 KHz. For a fixed phase relation between signal and reference, the same generator can be used for both inputs. To simulate a constant rate of phase change a separate generator can be used for the signal input. A frequency difference between the signal and reference, which is within the bandpass of the active low-pass filters, can be used when adjusting the level and hysteresis for the shaper. The level adjustment is adjusted for a symmetrical square wave at the output of the shaper. The hysteresis at the input to the shaper is adjusted for about ten percent of the peak input waveshape, with output of the shaper a symmetrical square wave. The function of the potentiometers are described below. The numbers used for the potentiometers are not consecutive.

Card No. 1

R-1 input signal level
R-2 signal presence threshold
R-3 input reference level
R-4 reference presence threshold
R-5 signal presence level
R-6 reference presence level

Card No. 2

R-8 center frequency adjustment for reference channel PLL
R-9 center frequency adjustment for signal channel PLL

Card No. 3

R-14 thru R-17 level adjustment for shapers
R-10 thru R-13 hysteresis adjustment for shapers

Card No. 6

DAC Adjustment

1. Remove chips 2, 3, and 4 on card no. 5.
2. Adjust R-2 and R-3 for -10V.D.C. ±2.44 mv.

3. Replace chips 3 and 4 on card no. 5.
4. Plug calibration header located on an unused socket at bottom of card no. 5 into socket 2.
5. Adjust R-1 +9.999 volts at the analog output while pressing the zero reset on the front panel.
6. Repeat 1 and check for -10 V.D.C. $\pm$2.44 mv.
7. Repeat 1 thru 6 if necessary.
8. Replace chips 2, 3, and 4 card no. 5 after the final adjustment.
9. For further information on the DAC HR 13B or AM101 amplifier consult the enclosed data sheets.

DEMONSTRATION TEST

A demonstration test of the LAM was conducted at NASA-Langley in the period from January 24 to February 2, 1979. The LAM equipment was installed in the 8-ft Transonic Pressure Tunnel and the system performance was checked over a wide spectrum of tunnel operational conditions. The test proved that the laser angle meter system will work over the required flow conditions.

The only problems encountered centered on the laser subsystem. There was one bad laser and one bad power supply. The defective laser was replaced early in the test. The defective power supply took more time, as the symptoms were intermittent. The laser power would drop to zero for about 100 milliseconds at random times, 15 minutes to two hours apart. The dropouts occurred mostly at low pressure. The wiring was checked for poor connections, the electronics were plugged into an independent 110 volt circuit, and the optical assembly was sealed and pressurized to one atmosphere, but the problem remained. An attempt was made to pressurize the laser power supply. Finally, the power supply was changed and the dropouts disappeared.

The first part of this section is a chronological description of the test, describing the problems that arose and the solutions attempted. The second part is a listing of the data from the NASA accelerometers and the Boeing LAM together with a discussion of the data.

Demonstration Test Log

1/24/79 - Checked equipment for shipping damage. Nothing broken, damaged, or misaligned. Set up system in IRD lab and ran a calibration at 1-degree intervals on reflectors 1 and 2. The results of a third order fit to the data are shown in Figures 15 and 16.

1/25/79 - Installed LAM at 8-ft tunnel.
1/26/79

1/29/79 - Wind tunnel crew installed model. Calibrated system from -6^{o} to $+16^{o}$ after model was in place.

1/30/79 - Started tunnel at 1300 hrs. Both signal and reference drop to zero for short periods. There appears to be a problem with the laser, laser power supply, or electrical connections to the optical assembly.
Shut down tunnel and changed the laser power supply.
No problems during run 1, M = 0.7, P_T = 2000. Interrupt light came on at 6^{o}, 12^{o}, and 14^{o} in run 2. The static pressure was 1/2 atmosphere. Set up scope to look at raw reference voltage and trigger on interrupt pulse. This showed that both signal and reference drop out together, indicating that the laser is going off. Several interrupts during runs 4 and 5. The static pressure was one-fourth of an atmosphere for both runs.
Installed new laser at end of shift.

1/31/79 - Clamped optical assembly in place and tied wiring down. The reference voltage is higher than before, but the signal is lower. This indicates some misalignment of the system, and may change the LAM calibration curve.
Run 6 - P_s = 1439, M = 0.7. The LAM came back to zero at the end of the run. No interrupts.
Run 7 - P_s = 1180, M = 0.9. No problem during run.
Run 8 - P_s = 579, M = 1.2. Several interrupts during run.

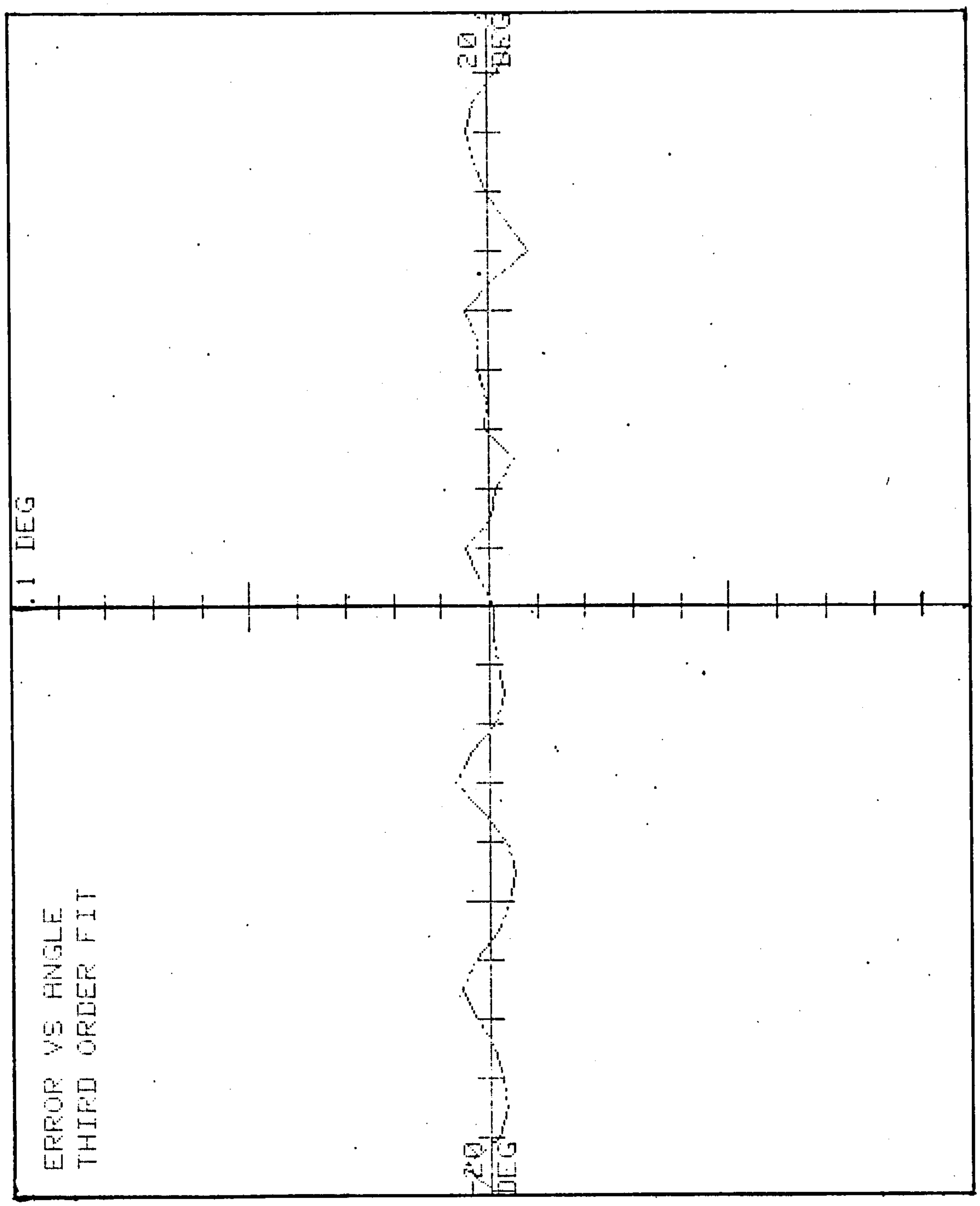

Figure 15- Calibration of retroreflector assembly No. 1

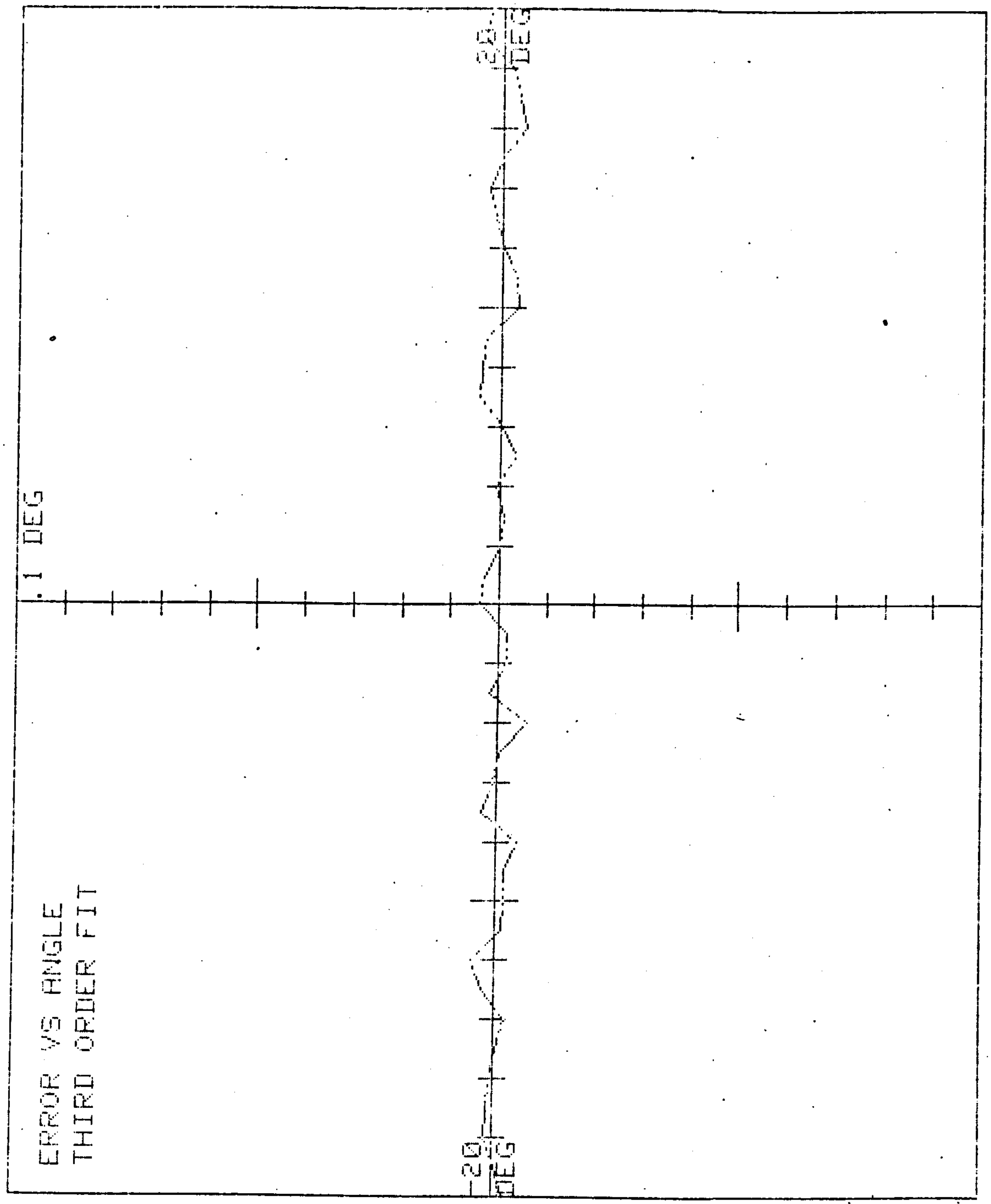

Figure 16– Calibration of retroreflector assembly No. 2

Run 9 - P_s = 1913, M = 0.25. Good run. Installed detector with separate power supply below optics for an independent check on laser operation.

Installed pressure fitting on optical assembly and attached to air line so unit can be held above static pressure.

Run 11 - P_s = 589, M = 1.2. Good run.

Run 12 - P_s = 1440, M = 0.7. One interrupt during run.

Run 13 - Started to decrease static pressure for run 13 and another interrupt occurred.

Run 14 - P_s = 1913, M = 0.25. Good run.

Run 14.5 - Wind off calibration at 2^o intervals

Run 15 - P_s = 2376, P_T = 3299, M = 0.7. High pressure run, no problems.

Run 16 - P_s = 4021, P_T = 4199, M = 0.25. Good run.

Run 17 - P_s = 2200, P_T = 2298, M = 0.25. Good run. After the system had operated okay for 2 1/2 hours at high pressure, the tunnel was pumped down to P_s = 842 and the interrupt light came on.

2/1/79 - Mounted laser power supply in a pressure vessel vented to the control room. The laser still dropped out at low pressure. After the run, it was found that the pressure vessel had not sealed properly. Two-part silicone rubber was used to seal both the optical assembly tube and the pressure vessel. When the pressure vessel was tested, the hinges and latch on the door failed at 10 psig, so attempts to pressurize the laser power supply were abandoned. The tunnel was turned on, with the optical assembly pressurized to one atmosphere. At one-half atmosphere static pressure the laser dropped out twice. The old laser power supply was reinstalled, so we now have a new laser with the original power supply.

Run 20 - P_s = 575, M = 1.2. Good run.

Run 21 - P_s = 1184, M = 0.9. Good run.

Run 22 - P_s = 1442, M = 0.7. Good run.

Run 23 - P_s = 1920, M = 0.25. Good run.

There have been no dropouts since the old power supply was installed. The new power supply was installed outside the plenum but not yet wired into the laser.

2/2/79 - Installed second new power supply in plenum and plugged laser in.
Run 24 - P_S = 576, M = 1.2. Good run.
Run 25 - M = 0.9. Good run. Wired laser into power supply outside plenum.
Run 26 - Very low pressure run, optical assembly vented to control room. P_S = 270, P_T = 650, M = 1.2. Good run.
Run 27 - P_S = 384, P_T 650, M = 0.9. Good run.
Run 28 - P_T = 650, M = 0.7. Good run.
Run 29 - P_T = 650, M = 0.25. Good run.

There have been no dropouts all day. Evidently the first laser we used was bad, and the second power supply could not operate at low pressure. Everything else operates properly.

Figure 17 is the calibration at the end of the demonstration test.

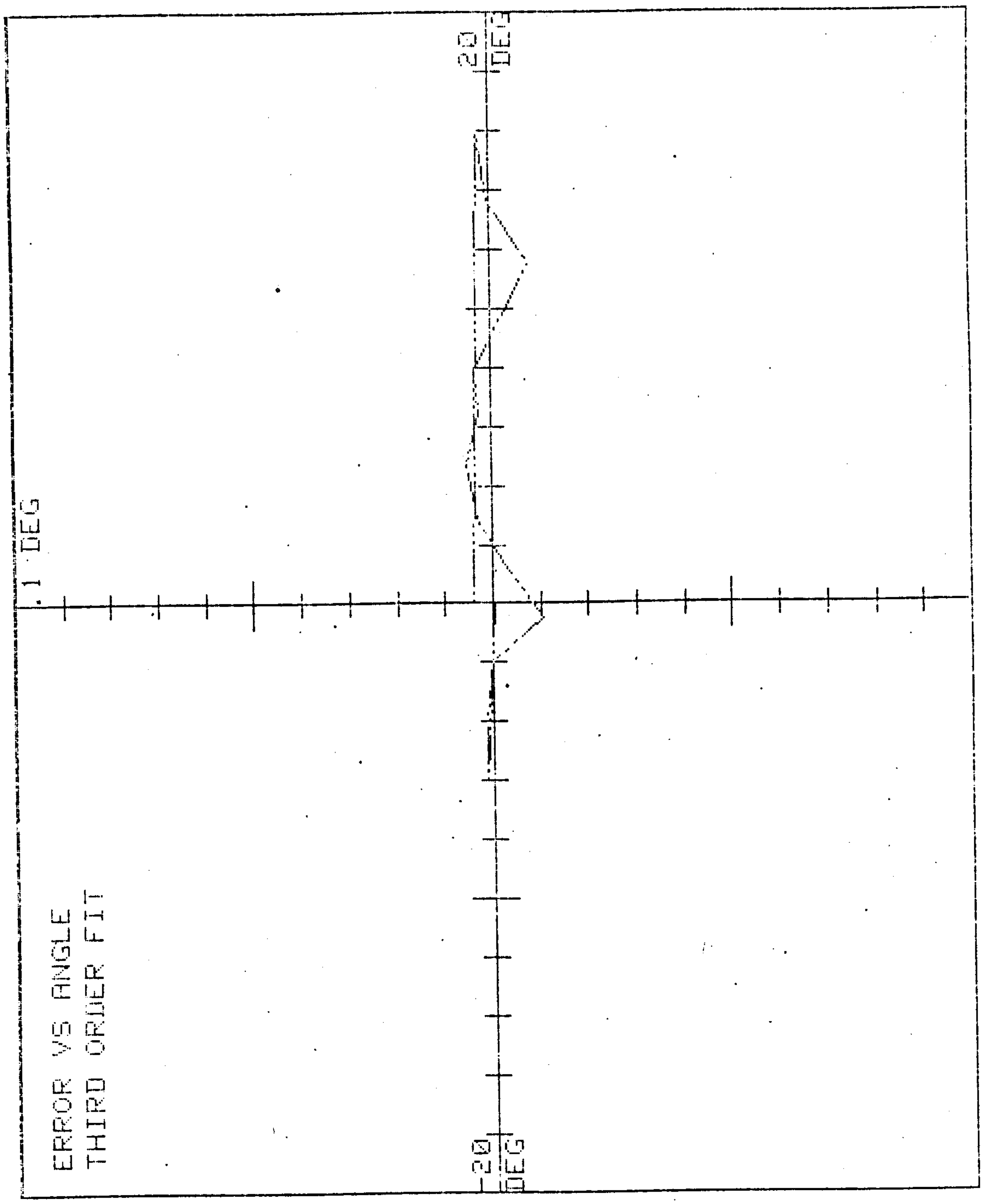

Figure 17- Calibration at end of test

Demonstration Test Data

Table 2 is a listing of the test data for the Kearfott and Q-Flex accelerometers and the Boeing laser angle of attack meter. The spread in the data is somewhat greater than expected from the initial calibration. Part of this is the result of changing lasers after the test was underway. The alignment of the new laser was not thoroughly checked because of time limitations. Calibration at the IRD lab at the end of the test showed this increased data spread, and the system has now been properly aligned. Another problem is that some of the LAM data was taken after the model had begun to pitch to the next angle. When this occurred, the fast response of the LAM resulted in a higher angular reading than the accelerometer readings.

The data in Table 2 is based on accelerometer sensitivities of:

$$S_k = 0.20032 \text{ v/g (Kearfott)}$$

$$S_q = 0.2854 \text{ v/g (Q-Flex)}$$

The final calibration shows that the numbers should have been:

$$S_k = 0.200486 \text{ v/g } (+ 0.083\%)$$

$$S_q = 0.285521 \text{ v/g } (+ 0.042\%)$$

Based on the final calibration, the angles in Table 2, columns 1 and 2, are high by 0.013^o and 0.007^o respectively at 16^o angle of attack.

The stability of the LAM was demonstrated during several long periods of consecutive runs, (Runs 14-17, 2.5 hrs; Runs 19-23, 2 hrs; Runs 24-25, 2 hrs; Runs 26-29, 2 hrs.) where there were no interrupts and the LAM reading returned to zero at the end of the mach series. This data also demonstrates the stability of the mounting assembly above the test section and the stability of the retroreflector assembly inside the model.

In conclusion, this test proved that the laser angle of attack meter will function throughout the range of pressure and flow conditions encountered

in the NASA-Langley 8-ft pressure transonic wind tunnel. As the system is used, other applications may become important, such as monitoring dynamic motion of the model to determine the onset of flutter and real-time angle measurement for automatic pitch control.

Table 2-a Test Data

	Kearfott	Q-Flex	Boeing
WIND OFF POST CAL	-4.989	-4.987	-4.985
	-3.560	-3.559	-3.562
	-2.382	-2.380	-.251
	-1.233	-1.231	-.243
	.027	.029	.022
	1.238	1.239	1.230
	2.413	2.414	2.410
	3.290	3.292	3.296
	4.484	4.486	4.492
	7.143	7.145	7.141
	8.582	8.584	8.580
	10.039	10.041	10.039
	11.535	11.536	11.534
	13.111	13.113	13.105
	15.025	15.028	15.016
	6.069	6.073	6.063
	1.973	1.977	1.966
	.543	.546	.537
	-.617	-.614	-.597
	-1.908	-1.905	-1.912
	-3.020	-3.017	-2.999
	-4.575	-4.572	-4.577
	-6.041	-6.038	-6.042
M=.7 Pt 2000 Run 1	-5.982	-5.978	-6.021
	-4.984	-4.979	-5.024
	-3.997	-3.992	-4.014
	-3.000	-2.996	-3.014
	-1.992	-1.987	-2.025
	-.004	.001	-.047
	.998	1.002	.951
	2.019	2.023	1.999
	2.997	3.001	2.965
	4.009	4.013	3.972
	5.017	5.019	4.969
	6.004	6.007	5.953
	7.986	7.987	7.943
	10.028	10.030	9.978
	11.995	12.000	11.946
	13.993	13.997	13.934
	16.056	16.058	16.008
	.012	.016	-.036

	Kearfott	Q-Flex	Boeing
M.95 Pt2000 RUN3	-6.012	-6.002	-6.023
	-4.977	-4.968	-4.976
	-4.013	-4.005	-4.027
	-2.945	-2.934	-2.981
	-1.990	-1.979	-2.011
	-.962	-.951	-1.003
	.002	.013	-.009
	1.013	1.022	.978
	2.008	2.016	1.985
	3.037	3.044	3.007
	3.979	3.984	3.957
	5.012	5.017	4.954
	5.990	5.993	5.690
	8.018	8.022	7.716
	10.009	10.028	9.716
	12.014	12.019	11.708
	14.013	14.034	13.228
	-.002	.005	-.077
M1.2 Pt1400 RUN4	-6.000	-5.979	-6.337
	-4.880	-4.851	-5.111
	-4.009	-3.984	-4.751
	-2.998	-2.974	-3.749
	-1.988	-1.966	-2.998
	-.998	-.982	.001
	.001	.015	.013
	1.010	1.025	1.029
	2.017	2.030	2.109
	3.010	3.025	3.097
	4.052	4.069	4.001
	5.003	5.010	4.878
	6.088	6.095	5.768
	6.922	6.937	6.469
	8.057	8.066	7.600
	-.010	.010	.334

Table 2-b Test Data

Run	Kearfott	Q-Flex	Boeing
M.25 Pt2000 RUN5	-6.005	-6.000	-6.059
	-5.003	-4.999	-5.053
	-3.993	-3.990	-4.026
	-2.998	-2.996	-3.034
	-2.001	-1.999	-2.048
	-1.017	-1.015	-1.065
	-.001	-.000	-.068
	1.001	1.001	.931
	2.015	2.015	1.967
	3.011	3.011	2.962
	3.993	3.992	3.936
	4.997	4.996	4.929
	5.999	5.997	.856
	8.007	8.004	2.875
	9.990	9.987	4.855
	9.993	9.989	4.854
	11.994	11.990	6.865
	13.991	13.985	8.863
	15.995	15.990	10.887
	-.005	-.004	-5.149
M.7 Pt2000 RUN6	-6.009	-6.005	-6.005
	-4.979	-4.976	-4.975
	-4.007	-4.005	-4.008
	-2.975	-2.973	-2.979
	-1.977	-1.974	-1.972
	-.977	-.976	-.983
	.032	.033	.029
	1.011	1.011	1.001
	2.022	2.022	2.017
	3.017	3.016	2.997
	4.015	4.014	3.987
	5.031	5.029	5.009
	6.009	6.007	5.988
	8.024	8.021	8.000
	10.040	10.036	10.011
	12.005	12.000	11.979
	14.042	14.037	14.015
	16.034	16.028	15.994
	.008	.007	.011
M.9 Pt2000 RUN7	-6.000	-5.998	-5.997
	-4.992	-4.991	-4.969
	-3.994	-3.994	-3.977
	-3.010	-3.010	-2.978
	-1.961	-1.960	-1.951
	-1.036	-1.035	-1.032
	-.009	-.010	.013
	.979	.976	.987
	2.032	2.030	2.029
	3.013	3.010	3.017
	4.027	4.026	4.015
	4.001	4.000	3.993
	5.017	5.015	4.993
	5.994	5.991	5.968
	8.028	8.029	8.007
	10.021	10.019	10.028
	12.059	12.061	12.048
	14.010	14.008	13.982
	.034	.033	.029
M.7 Pt2000 RUN12	-6.009	-6.002	-5.860
	-3.995	-3.989	-3.859
	-2.037	-2.032	-1.902
	.002	.005	.147
	2.027	2.029	2.160
	4.031	4.033	4.151
	6.028	6.029	6.161
	8.193	8.198	8.390
	8.035	8.035	8.159
	9.999	10.000	10.497
	12.004	12.003	12.518
	14.022	14.021	14.527
	15.980	15.974	16.471
	.003	.004	.019

Table 2-c Test Data

Run	Kearfott	Q-Flex	Boeing
M.9 Pt2000 RUN13	-5.995	-5.989	-5.979
	-3.996	-3.992	-3.978
	-1.913	-1.910	-1.884
	-1.989	-1.984	-1.949
	-.001	.002	.060
	2.043	2.046	2.084
	3.993	3.993	4.028
	6.007	6.007	6.038
	8.006	8.006	8.026
	9.924	9.924	10.643
	11.998	12.001	12.593
	14.032	14.034	15.040
	16.050	16.046	17.014
	.010	.012	-.052
M.25 Pt2000 RUN14	-6.026	-6.025	-6.010
	-3.999	-3.999	-3.983
	-2.017	-2.018	-2.011
	.004	.002	.019
	2.018	2.014	2.031
	3.999	3.994	3.998
	5.998	5.992	5.999
	8.030	8.023	8.031
	10.015	10.008	10.000
	12.017	12.007	12.016
	13.995	13.985	14.002
	15.992	15.981	15.971
	-.004	-.004	.008
WIND OFF RUN 14.5	-6.311	-6.310	-6.314
	-5.237	-5.237	-5.218
	-3.921	-3.921	-3.921
	-2.336	-2.338	-2.319
	-.450	-.453	-.432
	-.004	-.007	.008
	2.018	2.014	2.031
	3.975	3.971	3.983
	6.067	6.061	6.078
	7.978	7.972	7.992
	10.102	10.094	10.111
	12.057	12.049	12.062
	14.080	14.070	14.067
	16.006	15.995	15.990

Run	Kearfott	Q-Fl-x	Boeing
M.7 Pt3300 RUN15	-6.024	-6.017	-6.033
	-3.996	-3.990	-3.992
	-2.014	-2.008	-1.997
	.033	.041	.033
	2.018	2.022	2.001
	4.025	4.026	4.013
	6.060	6.064	6.047
	8.039	8.041	8.020
	10.050	10.051	10.022
	12.025	12.027	12.002
	14.005	14.007	13.975
	-.018	-.012	-.017
M.25 Pt4200 RUN16	-6.002	-6.001	-6.009
	-4.012	-4.012	-4.019
	-1.990	-1.991	-2.011
	-.005	-.007	-.016
	2.004	2.001	1.995
	4.011	4.007	3.986
	5.991	5.986	5.971
	8.038	8.032	8.018
	10.000	9.993	9.969
	12.033	12.025	12.019
	13.969	13.961	13.965
	16.007	15.999	15.988
	-.002	-.003	-.012
M.25 Pt2298 RUN17	-6.000	-5.998	-6.000
	-4.011	-4.011	-4.017
	-2.030	-2.031	-2.041
	-.019	-.021	-.033
	1.996	1.993	1.987
	4.007	4.003	3.985
	5.990	5.986	5.967
	7.990	7.985	7.978
	9.997	9.991	9.963
	11.995	11.988	11.977
	14.004	13.996	13.988
	16.003	15.994	15.963
	-.003	-.003	-.013

Table 2-d Test Data

Run	Kearfott	Q-Flex	Boeing
M1.2 Pt1400 RUN18	-5.997	-5.958	-5.500
	-3.998	-3.967	-3.503
	.007	.038	.547
	2.021	2.053	3.099
	4.010	4.038	4.993
	8.022	8.043	8.623
M.7 Pt2000 RUN19	-5.989	-5.976	-5.741
	-3.993	-3.982	-3.688
	.012	.023	.290
	2.038	2.048	2.385
	4.024	4.033	4.166
	8.018	8.026	8.209
	12.026	12.031	12.222
	16.047	16.051	16.199
M1.2 Pt1400 RUN20	-5.970	-5.938	-5.949
	-.371	-3.961	-3.982
	-1.978	-1.953	-1.971
	.013	.037	.024
	2.004	2.030	2.010
	4.027	4.055	4.015
	6.039	6.061	6.037
	8.022	8.049	8.010
	10.071	10.096	10.062
	.001	.034	.017

Run	Kearfott	Q-Flex	Boeing
M.9 Pt2000 RUN21	-6.005	-5.987	-5.992
	-4.001	-3.984	-3.991
	-2.016	-1.999	-2.004
	.025	.039	.046
	2.033	2.049	2.036
	4.001	4.016	4.004
	6.034	6.048	6.016
	8.020	8.035	8.013
	10.004	10.026	10.021
	12.017	12.041	12.015
	14.004	14.018	13.988
	16.034	16.049	16.019
	.019	.035	.023
M.7 Pt2000 RUN22	-6.016	-6.004	-6.012
	-4.013	-4.002	-4.011
	-2.018	-2.008	-2.025
	.009	.020	.070
	2.018	2.026	2.015
	3.993	4.000	3.979
	6.018	6.024	6.013
	8.003	8.009	7.993
	10.048	10.054	10.024
	12.008	12.011	11.993
	14.027	14.030	14.001
	15.981	15.984	15.950
	.013	.022	.016
M.25 Pt2000 RUN23	-5.999	-5.990	-5.995
	-4.010	-4.003	-4.010
	-1.986	-1.980	-1.998
	-.009	-.004	-.010
	1.990	1.994	1.989
	4.003	4.005	3.986
	5.996	5.997	5.985
	7.976	7.976	7.969
	10.020	10.019	9.993
	12.046	12.044	12.032
	14.014	14.010	13.998
	15.986	15.981	15.949
	-.022	-.017	-.032

Table 2-e Test Data

Run	Kearfott	Q-Flex	Boeing	Run	Kearfott	Q-Flex	Boeing
M1.2 Pt1400 RUN24	-6.000	-5.973	-5.967	M.9 Pt650 RUN27	-6.006	-5.998	-5.999
	-4.004	-3.972	-3.977		-4.018	-4.011	-4.010
	-2.025	-1.981	-1.990		-1.996	-1.989	-1.981
	-.004	.025	.028		-1.990	-1.984	-1.996
	.989	1.015	1.016		-.000	.005	.005
	1.983	2.003	1.997		2.101	2.112	2.223
	2.982	3.006	3.000		2.011	2.016	2.017
	4.297	4.329	4.457		4.000	4.004	3.989
	4.023	4.043	4.020		5.985	5.988	5.973
	5.015	5.033	5.010		7.939	7.944	7.930
	6.009	6.028	6.016		10.003	10.005	9.979
	7.006	7.023	7.011		-.004	.002	-.003
	8.019	8.037	8.011				
	-.003	.026	.029				
M.9 Pt2000 RUN25	-6.036	-6.018	-6.011	M.7 Pt650 RUN28	-5.992	-5.985	-5.981
	-3.958	-3.945	-3.955		-3.985	-3.980	-3.982
	-2.005	-1.994	-1.990		-1.999	-1.994	-2.006
	-.007	.002	-.011		.002	.006	.007
	2.001	2.009	2.017		2.020	2.023	2.024
	4.020	4.027	4.032		4.023	4.025	4.005
	6.019	6.025	6.038		6.020	6.022	6.012
	8.032	8.038	8.016		8.028	8.029	8.017
	9.997	10.004	10.017		10.013	10.013	9.987
	12.055	12.064	12.055		11.992	11.991	11.978
	14.035	14.039	14.026		14.013	14.009	13.999
	16.003	16.008	15.986		16.004	16.000	15.960
	.002	.010	.010		-.003	.001	-.001
M1.2 Pt600 RUN26	-6.006	-5.995	-5.997	M.25 Pt650 RUN29	-5.995	-5.989	-5.984
	-4.001	-3.989	-3.989		-4.021	-4.016	-4.011
	-2.011	-2.000	-2.012		-2.006	-2.002	-2.011
	-.005	.009	.002		-.002	.001	.002
	.992	1.003	1.002		2.008	2.010	2.014
	1.999	2.011	2.008		3.995	3.997	3.986
	2.996	3.009	2.999		6.020	6.021	6.021
	4.001	4.012	3.991		8.004	8.003	7.998
	5.027	5.035	5.010		9.998	9.996	9.973
	6.013	6.022	6.006		11.993	11.990	11.979
	6.998	7.006	7.000		13.984	13.980	13.978
	8.063	8.071	8.047		15.994	15.988	15.954
	.002	.015	.014		16.004	15.999	15.965
					.004	.009	.007

1. Report No.	2. Government Accession No.	3. Recipient's Catalog No.
NASA-159306		

4. Title and Subtitle	5. Report Date
LASER ANGLE MEASUREMENT SYSTEM	6. Performing Organization Code
7. Author(s) C. R. Pond, P. D. Texeira and R. E. Wilbert	8. Performing Organization Report No. D180-25234-1
	10. Work Unit No.
9. Performing Organization Name and Address Boeing Aerospace Company P. O. Box 3999 Seattle, WA 98124	11. Contract or Grant No. NASI-15410
12. Sponsoring Agency Name and Address National Aeronautics and Space Administration Washington DC 20546	13. Type of Report and Period Covered Contractor Report
	14. Sponsoring Agency Code

15. Supplementary Notes

Contract Monitor: Tom Finley, NASA Langley Research Center

16. Abstract

A laser angle measurement system was designed and fabricated for NASA Langley Research Center. The instrument is a fringe counting interferometer that monitors the pitch attitude of a model in a wind tunnel. A laser source and detector are mounted above the model. Interference fringes are generated by a small passive element on the model. The fringe count is accumulated and displayed by a processor in the wind tunnel control room. This report includes optical and electrical schematics, system maintenance and operation procedures, and the results of a demonstration test at the NASA-Langley 8-ft Transonic Pressure Tunnel.

17. Key Words (Suggested by Author(s))	18. Distribution Statement
Angle measurement Wind tunnel instrumentation Interferometry	Unclassified - Unlimited

19. Security Classif. (of this report)	20. Security Classif. (of this page)	21. No. of Pages	22. Price*
Unclassified	Unclassified		

N-305

For sale by the National Technical Information Service, Springfield, Virginia 22161

End of Document